THE STATISTICAL STRUCTURE OF SHORT RANGE FORECAST ERRORS AS DETERMINED FROM RADIOSONDE DATA PART I: THE WIND FIELD

A.Hollingsworth and P.Lönnberg
European Centre for Medium Range Weather Forecasts

ABSTRACT

This paper analyses the statistical structure of the errors of the short-range wind forecasts used in the global data assimilation system at ECMWF, by verifying the forecasts against radiosonde data over North America.

The theory of two-dimensional homogeneous turbulence is used to partition the perceived forecast errors into prediction errors which are horizontally correlated, and observational errors which are assumed to be horizontally uncorrelated. The theory further partitions the wind prediction errors into three components viz. large-scale, rotational and divergent components, and provides a spectral description of the covariance and cross-covariance functions for stream function and velocity potential. The calculations also provide an estimate of the vertical error covariance matrices for prediction error and for radiosonde observational error; by which we mean the combined effects of instrumental error and errors of representativeness.

The basic assumptions are that the forecast errors are horizontally homogeneous and that the observational errors are horizontally uncorrelated.

Several important results are found. The wind prediction errors are comparable in magnitude with the wind observation errors. The prediction errors are dominated by the synoptic scales, but there is a substantial large scale wind error which reverses phase between the stratosphere and troposphere. The synoptic scale errors are largely non-divergent in the troposphere. There are good grounds for increasing the resolution of the analysis system, both in the horizontal and the vertical.

1. INTRODUCTION

This paper analyses the statistical structure of the mid-latitude errors of the short-range wind forecasts used in the global data assimilation system at ECMWF, by comparing the forecasts with verifying radiosonde data over North America. As a by-product the method provides estimates of the observational error covariance matrices for radiosonde winds and heights. The structure of the height and the height-wind error covariances is analysed in a companion paper (Lönnberg and Hollingsworth 1985, referred to as Part II).

Observational data gives point information on forecast errors. Knowledge of the statistical structure of the forecast error is essential to make a good interpolation of the multi-variable observational information to a three-dimensional grid, so as to produce the analysis from which the next forecast can start. The statistical information is used in a variety of ways. It prescribes the length scales and spectra of the vertical and horizontal correlations and cross-correlations, it determines the extent and scale dependence of constraints such as non-divergence or geostrophy, and it determines the relative weights of different types of data and of the forecast model. In a different context, the statistical information plays a vital role in tuning the data-checking algorithms.

In addition to its function as an interpolation procedure, the optimum interpolation (O/I) analysis acts as a filter on the observational data. If $\underline{d}$ and $\underline{a}$ represent the vectors of observed and analysed values at a set of observation points, then one may write

$$\underline{a} = (\underline{\underline{P}} + \underline{\underline{O}})^{-1} \underline{\underline{P}}\, \underline{d}$$

where $\underline{\underline{P}}$ is the prediction error correlation matrix defined by the positions of the observations and the type of variable observed, and $\underline{\underline{O}}$ is the corresponding observation error correlation matrix, normalised by the

magnitudes of the prediction errors (Gandin 1963, Rutherford 1972, Schlatter 1975, Bergman 1979, Lorenc 1981).

If $(\underline{E}_i)$ are the eigenvectors of $\underline{\underline{P}}$, with eigenvalues λ_i, and if $\hat{a}_i$, $\hat{d}_i$ denote the projections of $\underline{a},\underline{d}$ on $\underline{E}_i$, then

$$\hat{a}_i = \frac{\lambda_i}{\lambda_i + \sigma^2} \hat{d}_i$$

provided the observational errors are random, uncorrelated, and of equal (normalised) amplitude σ^2 i.e. provided $\underline{\underline{O}}=\sigma^2 \underline{\underline{I}}$ where $\underline{\underline{I}}$ is the identity matrix. Results of this kind are well known in geophysical inverse theory (Zlotnicki et al. 1982).

This result clearly shows the filtering effect of the analysis. Components of the observed field with large eigenvalues are well analysed, while those components with small eigenvalues are damped. As discussed by the authors cited above, the filtering will be optimal, in the sense of optimally extracting all useful meteorological information from the observations while eliminating noise, if the prediction error structure functions are accurately determined from the forecast errors. An accurate and complete empirical determination of the forecast error and the observation error covariance functions is therefore essential (Seaman 1977).

Multivariate analysis constraints are widely used in current operational practice. As shown by Daley (1983), the imposition of constraints such as non-divergence or near-geostrophy can have a substantial effect on the resulting analysis by modifying the response characteristics of the analysis matrix. The present work presents results which justify some of the constraints used in current analysis algorithms, and indicates those aspects of current practice where change would be beneficial.

The operational optimal interpolation analysis system at ECMWF up to May 1984 used a Gaussian correlation for the height and stream function fields; it applied non-divergence and geostrophic constraints equally on all scales; and it fixed the horizontal scale of the structure functions through a single disposable parameter L_c. The statistical basis for much of the formulation was based on the results of Rutherford (1972) and Hollett (1975), together with a certain amount of empiricism. The resolution of the analysis was inadequate, especially in data rich areas, and there were important difficulties in the analysis of the large scale wind field in the tropics. One aim of the present work is to provide a sound statistical basis for a refinement of the analysis system, leading to more accurate analyses.

This paper uses the theory of two-dimensional turbulence to determine the correlation structure of the forecast errors in the wind field, subject only to the assumption of local homogeneity in the horizontal. The method partitions the wind forecast errors into rotational and divergent components, and provides a spectral description of the properties of the covariance and cross-covariance functions for stream function and velocity potential. In Part II a complete analysis of the height-stream function and height-velocity potential covariances is presented.

The main features of the results are that the forecast errors are comparable in magnitude with the observation errors, and that there are good grounds for increasing the resolution of the analysis system, both horizontally and vertically.

Section 2 discusses the assimilation system, and the data used for the study. The differential equations governing the wind-wind correlations are derived in Section 3. Computational aspects of the solutions are discussed in Section 4. Section 5 deals with the prediction errors and the observational errors of the wind field. Sections 6 and 7 discuss the horizontal and vertical structures of the non-divergent and divergent wind errors respectively. The results are reviewed in the final section.

2. THE ASSIMILATION SYSTEM AND THE STATISTICAL DATA

The assimilation system is an intermittent insertion system consisting of three main steps - the analysis step, the initialisation step, and the forecast step. The analysis system is described by Lorenc (1981) and is an application of the optimal interpolation technique discussed by Gandin (1963), Rutherford (1972), Schlatter (1975) and Bergman (1979). Similar methods are used in several operational centres (Gustavsson 1981). The notable feature of the ECMWF implementation is that the analysis is performed for a large number of grid-points and variables simultaneously, which requires the selection of a large quantity of data for each analysis volume. The demands on computer power are correspondingly large; a typical analysis requires the inversion of several thousand matrices with orders between 100 and 200.

The initialisation scheme is an application of the non-linear normal mode scheme proposed by Machenhauer (1977), and described by Temperton and Williamson (1981), and Williamson and Temperton (1981), and has been modified to include diabatic effects by Wergen (1982, pers.comm.).

The model used to produce the 6-hour forecast is the ECMWF grid-point model (Burridge and Haseler, 1977); the physical parameterisation package has been described by Tiedtke et al. (1979).

The ECMWF assimilation system has been used to produce global IIIb analyses for the FGGE year (Bjorheim et al. 1982, Bengtsson et al. 1982). The response of this and other assimilation systems to the FGGE level II-b data has been compared in Hollingsworth et al. (1985b) and Arpe et al. (1985).

The data studied here are the differences between the observations and the 6-12 hour grid-point model forecasts for the period 1 January-30 March, 1983. Only radiosonde data for 1200GMT is used; a particular station is used only if a minimum of 60 acceptable reports were available from the station. Acceptable means that the data was accepted as probably correct by all the stages of the operational quality control procedure. Attention is concentrated on the North American region between 30°N and 60°N. Later papers will consider results for other regions.

The mean difference between the station reports and the forecast is removed separately for each station. The average variance of the resulting ensemble of station time series is defined as the ensemble mean of the station variances. We use the notation $\langle a,b \rangle$ for the correlation of a with b, $\mathrm{cov}\langle a,b \rangle$ for the covariance and E_a, E_b for the standard deviations so that

$$\mathrm{cov}\langle a,b \rangle = E_a E_b \langle a,b \rangle$$

For vectors, we use the notation $\mathrm{cov}\langle \underline{c}.\underline{d} \rangle$ to denote the sum of the cross-covariances of their components. We say 6-12 hour forecasts for the same reasons as Hollett. Satellite data was not used over land below 100 mb, and Airep data is unavailable over land. The data input in the analyses over North America consisted of Synops and Temps at 0000 and 1200 GMT, but only Synops at 0600 and 1800 GMT. Since the Synop data mainly affects the lower troposphere, it is unclear whether the forecasts for the upper troposphere and lower stratosphere should be called 6-hour or 12-hour forecasts.

3. THE STATISTICAL STRUCTURE OF THE WIND FIELD ERRORS

3.1 Covariances of height and wind

In most current implementations of statistical analysis (O/I) it is assumed that the $\langle\phi,\phi\rangle$ and $\langle\psi,\psi\rangle$ prediction error auto-correlations are identical, that the $\langle\chi,\chi\rangle$ correlation is identically zero, and that the $\langle\phi,\psi\rangle$ correlation can be expressed in a single geostrophic coupling parameter, μ, which may vary with latitude (Bergman 1979, Lorenc 1981); (here ϕ, ψ, χ represent the geopotential, stream function and velocity potential). As discussed by Daley (1983), a complete representation of the error field requires six correlation functions: $\langle\phi,\phi\rangle$, $\langle\psi,\psi\rangle$, $\langle\chi,\chi\rangle$, $\langle\phi,\psi\rangle$, $\langle\phi,\chi\rangle$, $\langle\psi,\chi\rangle$ plus three variances. If the statistics are horizontally inhomogeneous, then each of the correlations is a function of six variables $(x_1,y_1,p_1;\ x_2,y_2,p_2)$. If one assumes horizontal homogeneity then they are functions of four variables $(r,\theta,\ p_1,p_2)$, where r,θ are the polar coordinates of the displacement vector between the two points; the isotropic component is a function of 3 variables (r,p_1,p_2). The verification of the forecasts against the radiosonde data enables one to calculate the correlation functions $\langle\phi,\phi\rangle$, $\langle u,u\rangle$, $\langle v,v\rangle$, $\langle u,v\rangle$, $\langle\phi,u\rangle$, $\langle\phi,v\rangle$. From these functions one may calculate the six correlation functions involving ϕ, ψ, χ by solving the differential equations which relate one set to the other. The generality introduced by Daley is needed for a complete understanding of the forecast error structures.

3.2. Mathematical formulation of the homogeneous problem

To discuss the statistical structure of the forecast errors in the wind field we apply the formulation introduced by Daley (1983) to general homogeneous conditions. From the relationships

$$u = -\psi_y + \chi_x \text{ and } v = \psi_x + \chi_y, \tag{3.1}$$

expressions in terms of the stream function, velocity potential and their cross-correlation are introduced as follows

$$\gamma^2 \langle \psi,\psi \rangle = F(r,\theta)$$

$$\delta^2 \langle \chi,\chi \rangle = G(r,\theta) \qquad (3.2)$$

$$\gamma\delta \langle \psi,\chi \rangle = H(r,\theta)$$

so that, by analogy with Daley (1983)

$$\langle u,u \rangle = -(F_{yy}+G_{xx}-2H_{xy})$$

$$\langle v,v \rangle = -(F_{xx}+G_{yy}+2H_{xy}) \qquad (3.3)$$

$$\langle u,v \rangle = (F_{xy}-G_{xy}-H_{xx}+H_{yy})$$

This implies that γ^2 and δ^2 are the fractions of the synoptic scale vector wind prediction error variance arising from the non-divergent and divergent wind respectively, each multiplied by the square of the corresponding component length scale (see Sect. 4.4). This is another way of saying that $\gamma = E_\psi/E_\ell$, $\delta = E_\chi/E_\ell$ where E_ψ, E_χ, E_ℓ are the rms amplitudes of ψ, χ, and the synoptic scale wind component.

The second derivatives of F,G,H are therefore non-dimensional; the use of the component length scale rather than the turbulent microscale simplifies the algebra.

A necessary consequence of homogeneity is that $\langle u,v \rangle = \langle v,u \rangle$; this therefore suggests a test for homogeneity. Adding and subtracting the first two relations one can cast the equations in the more symmetrical form

$$\langle u,u \rangle + \langle v,v \rangle = -\nabla^2(F+G)$$

$$\langle u,u \rangle - \langle v,v \rangle = -\left(\frac{\partial^2}{\partial y^2} - \frac{\partial^2}{\partial x^2}\right)(F-G) + 4\frac{\partial^2 H}{\partial x \partial y} \qquad (3.4)$$

$$\langle u,v \rangle = \frac{\partial^2}{\partial x \partial y}(F-G) + \left(\frac{\partial^2}{\partial y^2} - \frac{\partial^2}{\partial x^2}\right)H$$

where ∇^2 is the Laplacian. As noted by Buell (1972) the sum $\langle u,u\rangle+\langle v,v\rangle$ is a scalar, being the trace of the velocity correlation matrix, and is therefore invariant under coordinate transformations. This suggests that the equations be transformed to polar coordinates, using the longitudinal and transverse velocity components. The equations (3.4) then become

$$\begin{aligned} -\nabla^2(F+G) &= \langle \ell,\ell\rangle + \langle t,t\rangle \\ L_1(F-G)-4L_2(H) &= \langle \ell,\ell\rangle - \langle t,t\rangle \\ L_2(F-G) + L_1(H) &= -\langle \ell,t\rangle \end{aligned} \tag{3.5}$$

where $\nabla^2 = r^2R^2 + 2R + T^2$, $\quad R = \frac{1}{r}\frac{d}{dr}$, $\quad T = \frac{1}{r}\frac{d}{d\theta}$

$$L_1 = r^2R^2 - T^2$$

$$L_2 = T(\frac{1}{r} - rR)$$

ℓ,t are the longitudinal and transverse components of velocity, parallel to and orthogonal to the direction between two measurement points.

These are the partial differential equations for two-dimensional homogeneous turbulence. The radial derivatives of the empirical correlations tend to zero at large separations, so it is reasonable to pose expansions for the unknowns F, G, H in terms of cylindrical harmonics

$$F = \sum_m \begin{matrix}\cos\ m\theta \\ \sin\ m\theta\end{matrix} \sum_n F_{mn}\, J_m\,(k_{mn}\, r/D)$$

where the wavenumbers k_{mn} are specified by zero derivative boundary conditions at r=D, where D is some conveniently large number. Approximate solutions for F,G and H are then readily found by specifying the truncation of the series, and finding a least squares fit to the empirical velocity correlation data on the right of (3.5). These computational considerations are discussed in Section 4.

3.3 The isotropic problem

The equations for the isotropic component are derived by assuming that $\frac{\partial}{\partial\theta} = 0$ in (3.5):

$$\begin{aligned} -(r^2R^2 + 2R)(F+G) &= \langle \ell,\ell \rangle + \langle t,t \rangle \\ r^2R^2(F-G) &= \langle \ell,\ell \rangle - \langle t,t \rangle \\ -r^2R^2H &= \langle \ell,t \rangle \end{aligned} \qquad (3.6)$$

If one assumes that the error wind field is purely rotational then the equations (3.6) degenerate into one equation for the $\langle \psi,\psi \rangle$ correlation, together with two consistency conditions on the wind-wind correlations, which must be simultaneously satisfied. The consistency conditions have been discussed by Buell (1972), and a similar set of conditions is presented in Panchev (1971). Brown and Robinson (1979) have used the assumption of non-divergence in this form to estimate the spectrum of the wind field from radiosonde observations.

The first two equations of (3.6) may be added and subtracted to yield the equivalent form

$$\begin{aligned} -RF - (r^2R^2+R)G &= \langle \ell,\ell \rangle \\ -(r^2R^2+R)F - RG &= \langle t,t \rangle \\ -r^2R^2H &= \langle \ell,t \rangle \end{aligned} \qquad (3.7)$$

where the isotropic component of the observed velocity correlations is implied on the right hand sides.

The equations (3.7) subsume as special cases two well known results in the theory of homogeneous turbulence. If the flow is non-divergent then $\delta = H = G = 0$, and the velocity correlation tensor is determined by the single function F. The longitudinal and transverse correlations are related to F by

$$\begin{aligned} -RF &= \langle \ell,\ell \rangle \\ -(r^2R^2+R)F &= \langle t,t \rangle \end{aligned} \qquad (3.8)$$

Elimination of F leads to the well-known differential relation between the longitudinal and transverse correlations of incompressible isotropic turbulence (von Karman and Howarth 1938), due allowance being made for the difference between two and three dimensions (Obukhov 1954, Hutchings 1955).

In a symmetrical way, if the flow is irrotational, then $\gamma=H=F=0$ and the velocity correlation tensor is determined by the single function G. Then the longitudinal and transverse correlations are given by

$$-(r^2R^2+R)G = \langle \ell,\ell \rangle \qquad (3.9)$$

$$-RG = \langle t,t \rangle$$

Elimination of G leads to the differential relation between the longitudinal and transverse correlations of irrotational isotropic turbulence (Obukhov 1954), due allowance again being made for the difference between two and three dimensions.

Obukhov (1954) showed that if a three-dimensional random field consisting of both solenoidal (non-divergent) and potential (divergent) velocities is homogeneous and isotropic, then the solenoidal and potential components of the flow are uncorrelated. A simple extension of his argument shows that the same result applies in two dimensions. However, as pointed out by Panchev (1971) the conditions of the theorem are strict, as they require not only homogeneity and isotropy of the solenoidal and potential velocity fields, but also invariance of their joint correlation functions and tensor moments to a complete set of translations, rotations and reflections. Hence there is no inconsistency in positing a joint correlation, H, between the isotropic components of the ψ and χ forecast errors, as we have no a priori information about their joint correlation.

3.4 The anisotropic components

The isotropic component of the forecast error is familiar from earlier studies (Rutherford 1972, Hollett 1975). The anisotropic part has not received as much attention from those engaged in numerical weather prediction. The corresponding components of the climatological fields have been the subject of many studies (Buell 1971, Panchev 1971, Julian and Thiebaux 1975, Buell and Seaman 1983). By definition a homogeneous auto-correlation function must be periodic in the azimuthal coordinate, with period π. Thus auto-correlations of variables on the same horizontal level must be expanded in Fourier-Bessel series using only even azimuthal harmonics. This restriction does not apply for correlations between variables at different levels, or different variables at the same level, and such expansions will generally require all the azimuthal harmonics. It is easy to see that the m=1 components can describe the vertical tilt of the forecast errors, while the m=2 components can describe correlations which are elongated along a certain horizontal direction, and therefore have an elliptic character. The anisotropic components will be the subject of a later study.

3.5 Separation of prediction and observation error

Given the isotropic part of the representation, one may extrapolate the horizontal correlation for perceived forecast error to zero separation, and so estimate the random observation errors for the radiosondes, which are assumed to be horizontally uncorrelated and of uniform magnitude (Hollett 1975). This is a good assumption, and is widely used in this type of work. It should be clearly understood that the observational error derived in this way includes both instrumental error and errors of representativeness, also known as sampling errors.

3.6 Multilevel correlations

In addition to determining the horizontal correlations of forecast errors for winds at the same levels, one may determine the horizontal and vertical error correlations by solving equations of the form (3.4) for the thermal wind errors for all possible combinations of levels. The extrapolation of these expressions to the origin enables one to partition the vertical covariance matrix into observational and prediction error parts. To see this, let

$\Delta\underline{e}_i, \Delta\underline{e}_j$ denote the vertical difference between the perceived wind forecast errors $\underline{e}_1$, $\underline{e}_2$, at horizontal points i,j and levels 1 and 2;

$\Delta\underline{p}_i$, $\Delta\underline{p}_j$ denote the corresponding prediction errors;

$\Delta\underline{b}_i$, $\Delta\underline{b}_j$ denote the corresponding observation errors.

Then the correlation of the perceived thickness or thermal wind error may be expanded as

$$\text{cov}\langle\Delta\underline{e}_i \cdot \Delta\underline{e}_j\rangle = \text{cov}\langle(\Delta\underline{p}_i + \Delta\underline{b}_i).(\Delta\underline{p}_j + \Delta\underline{b}_j)\rangle$$

$$= \text{cov}\langle\Delta\underline{p}_i.\Delta\underline{p}_j\rangle + \text{cov}\langle\Delta\underline{b}_i.\Delta\underline{b}_j\rangle\delta_{ij} \qquad (3.10)$$

Given the functional representation of the isotropic part of the wind shear covariance, one may extrapolate to the origin and derive the prediction error and observation error for the wind difference between levels 1 and 2. This algorithm is applied for all possible pairs of levels 1 and 2. One can then derive the vertical covariance matrix for the observation error and prediction error of wind, given that the relevant variances have been calculated already at each level.

Since the wind difference between two layers is a vector quantity, the use of the equations in this way is a legitimate procedure provided the assumption of homogeneity is valid for the wind shears between layers.

This method of splitting the vertical covariance matrix into its observational and prediction components is quite different from the method used by Hollett (1975). Hollett used the simplifying, but unjustified, assumption that the prediction and observation covariance matrices had the same eigenvectors.

3.7 Discussion

The equations of two-dimensional turbulence introduced by Daley (1983) for the study of forecast errors have been transformed in a way which clarifies the physics of the problem and simplifies computation. The transformation also shows that several well-known results in the theory of isotropic turbulence are special cases of the equations used here. The equations can be used to derive the three-dimensional isotropic and anisotropic auto- and cross-correlations of ψ and χ from empirical data on the two-point velocity correlation tensor. In addition the vertical covariance matrix for radiosonde observational errors is readily found.

4. COMPUTATIONAL CONSIDERATIONS IN THE DETERMINATION OF PREDICTION AND OBSERVATION ERRORS

In this section we discuss the computational considerations involved in the determination of the prediction errors and observation errors for the wind field.

4.1 Method of solution and positive definiteness

As usual when discussing the statistical structure of forecast errors one assumes that the errors are homogeneous. Even if the covariance functions are inhomogeneous, the corresponding correlation functions are frequently more homogeneous, as noted by Panchev (1971, p311), Rutherford (1972), and Julian and Thiebaux (1975). Where possible, we work with the correlation functions. The question of homogeneity is discussed further in Part II.

Given the assumption of homogeneity, a two-point correlation $F(x_1,y_1;x_2,y_2)$ is a function only of the displacement between the points, and may be expressed as $F(r,\theta)$, where

$$r = [(x_1-x_2)^2 + (y_1-y_2)^2]^{\frac{1}{2}}$$

$$\theta = \tan^{-1}\left[\frac{y_2-y_1}{x_2-x_1}\right]$$

According to standard theory (Khinchin (1934), Batchelor (1953), Gandin (1963), Buell (1971,1972), Rutherford (1972)) the necessary and sufficient condition that $F(r,\theta)$ should be the auto-correlation function of a homogeneous random process is that F should be expressible in the form

$$F = \int \hat{F}(k)\, \exp(i\underline{k}.\underline{r})dk$$

where $\hat{F}(k)$ is square integrable and positive semi-definite. In two dimensions

the Fourier transform can be re-written as a Hankel transform (Gandin 1963, Rutherford 1972) so that

$$F(r,\theta) = \sum_m a_m(r) \cos m\theta + b_m(r) \sin m\theta \qquad (4.1)a$$

where $a_m(r), b_m(r)$ are expanded in Bessel functions as

$$a_m(r) = \sum_n A_{mn} J_m(k_{mn} r) \qquad (4.1)b$$

$$b_m(r) = \sum_n B_{mn} J_m(k_{mn} r) \qquad (4.1)c$$

A typical calculation begins with determining the empirical values of a particular correlation for all possible pairs of stations. The correlation data is then composited using the assumption of homogeneity. If necessary for reasons of space, the correlations may be averaged over distance intervals or 'bins' as discussed below. A least squares procedure is used to fit a Fourier-Bessel series, or a derivative of a Fourier-Bessel series, to the empirical correlation data. The condition of positive definiteness for an auto-correlation then becomes a requirement that the expansion coefficients should be positive in the isotropic part of the expansion, and that the implied phase functions should be continuous in the anisotropic part of the expansion. For the truncated Fourier-Bessel expansion, boundary conditions must be specified at some finite distance D; these are discussed later. For the moment all we need is that the basis functions should be complete and orthogonal.

(a) Coordinate systems

In discussing the statistical properties of forecast errors on a sphere, we use spherical geometry to calculate distances and directions. When dealing with the autocorrelation functions of homogeneous isotropic processes on the sphere one should use the Legendre functions as basis functions

(Obukhov 1954). Since one is dealing here with rather small areas, of typical dimension 3000 km, Fourier-Bessel series expansions rather than spherical harmonic expansions are used for computational convenience. The effects of sphericity are nevertheless fully accounted for in the representation.

(b) Averaging of correlations

In many of the calculations the correlations are averaged over certain distance ranges or bins. In calculating these bin averages, Fisher's z-transform is used (Fisher 1921). This procedure has the property that it preserves the distribution of the correlations about their local mean.

To test the stability of the calculations, some of the more sensitive quantities were calculated with the bin-width varying between 10 and 100 km. A variation of the averaging width between these limits produced a 1% change in the value of the coefficient of the 10'th mode of the height correlation. In this, as in most other features of the calculations, the stability of the calculations was quite satisfactory.

4.2 Boundary conditions

The choice of boundary conditions to be applied to the representation determines the wavenumbers k_{mn}. It is convenient to impose the boundary conditions that the radial derivatives of the $\langle\psi,\psi\rangle$, $\langle\chi,\chi\rangle$ and $\langle\psi,\chi\rangle$ correlations are zero at a sufficiently large distance D, which is determined in practice by requiring that the wind-wind correlations are essentially zero for $r>D$.

The correlations involving the wind become very small for station separations greater than 1500 km. The parameter D may be thought of as a truncation parameter for the analysis system, defining the diameter of the data search volume. As discussed by Phillips (1982) an ideal data selection algorithm would use all observational data in a single calculation. Since this is not feasible, some compromises have to be made in practical analysis schemes. The fact that the correlations involving the winds are small for separations larger than 1500 km suggests that the data search radius should be 1500 km. If this is adopted then one needs to be able to calculate correlations over twice this distance. A value of 3000 km is therefore used for D.

This suggestion accords reasonably well with our current practice. In analysing a volume of horizontal dimension 660 km, a search for data is made as far as 1200 km from the edge of the box, if closer data cannot be found. This limit was originally chosen because with a Gaussian structure function (L_c=600 km) for height and wind, the correlation between an observation at the centre of the box and an observation at the limit of the search radius is rather small; moreover experience showed that this search radius stretched computer resources to the limit. With this boundary condition the leading term in the isotropic part of the expansion is a constant term independent of r. It represents the mean value of the correlation over the domain (Hildebrand 1962,p227).

The choice of the truncation parameter D has a number of important consequences for the analyses, both from a practical and from a theoretical point of view. For a scalar variable like height, the local analysis can

respond to information in the data on scales between the upper bound of resolved scales (dependent on D), and the lower limit of resolution which is determined by the smallest inverse wavenumber k_N^{-1} which is retained in the truncated expansion, and by the data density. Information on scales larger than the upper bound will be mainly projected on the constant term, which physically corresponds to errors in the mean height over the selection area. Just as for the height field, the constant term in the wind-wind correlations occurs because there are components of the wind forecast errors which are of such large scale that they are essentially constant over a domain of dimension D. If $\ell = \ell_o + \ell_s$, $t = t_o + t_s$

where the subscripts o,s denote the large-scale and synoptic components respectively, then

$$\text{cov}\langle \ell, \ell \rangle = \text{cov}\langle \ell_o^2 \rangle + \text{cov}\langle \ell_s, \ell_s \rangle$$

$$\text{cov}\langle t, t \rangle = \text{cov}\langle t_o^2 \rangle + \text{cov}\langle t_s, t_s \rangle$$

Because of the truncation of the diameter of the selection radius to D, there are large-scale components in the wind correlations which have no corresponding term in the stream function or velocity potential correlations. It follows that the derivations in Section 3 are applicable only to the synoptic scale components. The large scale components must be accounted for in the least square calculations, but they do not enter the differential relations between the variables.

4.3 Degrees of separability

A vertical correlation matrix may be defined separately for each term in the horizontal expansion, i.e. for each horizontal mode. For the isotropic component of the errors one may write for a variable f (which may be ψ or χ)

$$\mathrm{cov}\langle f_{ik}, f_{jl}\rangle = E^f_k \; E^f_l \sum_{n=o}^{N} (A^f_{kn} \; A^f_{ln})^{\frac{1}{2}} \; C^f_n(k,l) \; J_o(k_n \; r_{ij}/D) \qquad (4.2)$$

where E^f_k, E^f_l are the forecast errors at levels k,l, and $C^f_n(k,l)$ is the vertical correlation matrix for mode n; k and l index the vertical levels, i and j index the horizontal position. The horizontal covariance of the error of the wind is determined for all levels, while the covariance of the error of the vertical wind difference is determined for all pairs of levels. Extrapolation to the origin then gives all the covariances required to define the vertical covariance matrix of each horizontal mode. The average correlation is therefore a weighted average of the correlations of the separate modes.

If the vertical correlation matrices $C^f_n(k,l)$ are independent of the modal index, and are all equal to $C^f(k,l)$, then the expansion may be written

$$\mathrm{cov}\langle f_{ik}, \; f_{jl}\rangle = E^f_k \; E^f_l \; C^f(k,l) \sum_{n=o}^{N} \left(A^f_{kn} \; A^f_{ln}\right)^{\frac{1}{2}} \; J_o(k_n \; r_{ij}/D). \qquad (4.3)$$

If, in addition, the coefficients $A_n(k,l)$ are the same for all levels and all combinations of levels, then the expansion is fully separable as

$$\mathrm{cov}\langle f_{ik}, \; f_{jl}\rangle = E^f_k E^f_l \; C^f(k,l) \sum_{n=o}^{N} A^f_n J_o(k_n \; r_{ij}/D) \qquad (4.4)$$

Current implementations of statistical interpolation analysis assume formulations of the latter kind. The validity of the separability assumptions can be tested by examining the variation of the normalised spectrum with level, and the variation of the vertical correlation with horizontal mode.

The data do not immediately justify an assumption of homogeneity in the vertical. This means that, in principle, a distinct horizontal function is needed to represent the functional dependence of the spatial correlation for each pair of levels. It turns out that homogeneity of the correlations in the vertical is a reasonably good approximation, provided the levels are sufficiently close to each other.

4.4 Length scales of the correlation functions

It is useful to define a horizontal length scale for the correlation functions. For each term in the isotropic horizontal expansions (4.1)a,b there is the relation

$$\nabla^2 J_o(k_n r/D) = - \left(\frac{k_n}{D}\right)^2 J_o (k_n r/D)$$

For the spherical harmonic functions there is the analogous relation

$$\nabla^2 Y_m^\ell = - \frac{m(m+1)}{a^2} Y_m^\ell$$

where Y_m^ℓ is a spherical harmonic, m is the total spherical wave-number and a is the radius of the earth. For each radial wavenumber k_n, one may define an equivalent spherical total wavenumber K_n such that

$$\left(\frac{k_n}{D}\right)^2 = \frac{K_n(K_n+1)}{a^2}$$

This equivalent spherical wavenumber K_n will be used to label the wavenumber axis on plots of spectra or normalised spectra.

Table 1. Values of $k_n, K_n, D/k_n, L_c, L_k$ for the isotropic modes.

n	k_n	K_n	D/k_n (km)	L_c (km)	L_k (km)
0	0	0	∞	∞	∞
1	3.8	8	789	1116	4957
2	7.0	15	429	607	2695
3	10.2	22	294	416	1847
4	13.3	28	226	312	1420
5	16.5	35	182	257	1143
6	19.6	42	153	216	961
7	22.8	49	132	187	829
8	25.9	55	116	164	729
9	29.0	62	103	146	647
10	32.2	68	93	131	584

Table 1 shows k_n, K_n, D/k_n, $L_c = \sqrt{2}(D/k_n)$, and $L_k = 2\pi D/k_n$, for the isotropic problem. The quantity D/k_n provides a convenient definition of the scale of each of the horizontal modes. To define the scale of a correlation function, one proceeds in an analogous fashion, so that the scale L_f of a function F is defined as

$$L_f^2 = - \left(\frac{F}{\nabla^2 F}\right)_{r=0}$$

This is equivalent to the definition of the microscale in turbulence theory. If F is isotropic with expansion coefficients F_n then the scale of F is defined by

$$L_f^2 = D^2 \frac{\Sigma F_n}{\Sigma k_n^2 F_n}$$

and corresponds to a spectrally weighted average of the scales of the constituent modes of F.

If F is a stream function (or a velocity potential), then the length scale so defined gives the ratio of the stream function (or velocity potential) variance to the sum of the variances of the two velocity components, i.e. the associated vector wind variance. The 'component' length scale L_c is the length scale which defines the ratio of the stream function (or velocity potential) amplitude to the corresponding rms velocity component. In several operational systems a Gaussian is used for the auto-correlation functions in the form (Bergman 1979, Lorenc 1981)

$$F(r) = \exp\left[-\tfrac{1}{2}\left(\frac{r}{L_c}\right)^2\right]$$

The rms velocity component E_t associated with F is given by

$$E_t = \frac{E_F}{L_c}$$

Since the authors just cited work with the wind component error rather than the vector wind error, there will be a factor of $\sqrt{2}$ difference between their definition of the length scale and ours. One may think of L_c as an approximate quarter wavelength for the exponential.

4.5 Discussion

The least-squares solution of the turbulence equations requires the specification of a truncation parameter for the analysis system corresponding to the diameter D of the data selection area. The choice of D/2 as a distance beyond which all the wind-wind correlations are zero leads to a consistent set of boundary conditions for the turbulence equations. The natural basis

functions for the problem contain a function corresponding to a time-varying wind error which is constant over the data selection area. It is likely that the neglect of such a term in our pre-1985 operational analysis system contributes to the problems in the analysis of the large-scale tropical wind field noted by Cats and Wergen (1982). Given a complete set of basis functions the solutions are readily found, once the truncation of the series expansions has been decided.

5. THE PREDICTION AND OBSERVATION ERRORS FOR WIND

5.1 The isotropic component of the total wind error

The series expansions of the solutions of equations (3.6) must be terminated when a coefficient becomes negative, if the solution is to satisfy the requirement of positive-definiteness. One therefore needs to consider the desirability of using the full truncation that is computationally available.

Fig. 1 shows the empirical data on the radial distribution of the isotropic part of the 500 mb $\langle u,u\rangle+\langle v,v\rangle$ correlation, together with the least-squares fitting curves derived using 6, 8, 10, 12 and 14 terms in the expansion for the spatial correlation of the total wind. As the truncation wavenumber is increased, the perceived error variance on the shorter scales is better resolved and so is treated as horizontally correlated prediction error rather than horizontally uncorrelated observational error, where the term observation error includes both instrumental error and errors of representativeness. If one were using low truncation structure functions in the analysis algorithm of this assimilation system, then one would have to recognise that the observation error, in this definition, must be horizontally correlated (M.Pedder, pers.comm.).

Fig. 2 shows the 500 mb spectra for the total wind error, for truncations at even numbers between 6 and 14. The calculations are remarkably stable. A feature of the results is the increase in amplitude at all wavelengths, as the truncation is increased. This would not happen if the basis functions were orthogonal on the grid defined by the data points. A comparison of Figs. 1 and 2 suggests that the correlation of the total wind error is negligible for distances much larger than 1000 km, and that increases in the truncation are quite stable, as far as we have gone, because of the sharpness of the correlations near the origin.

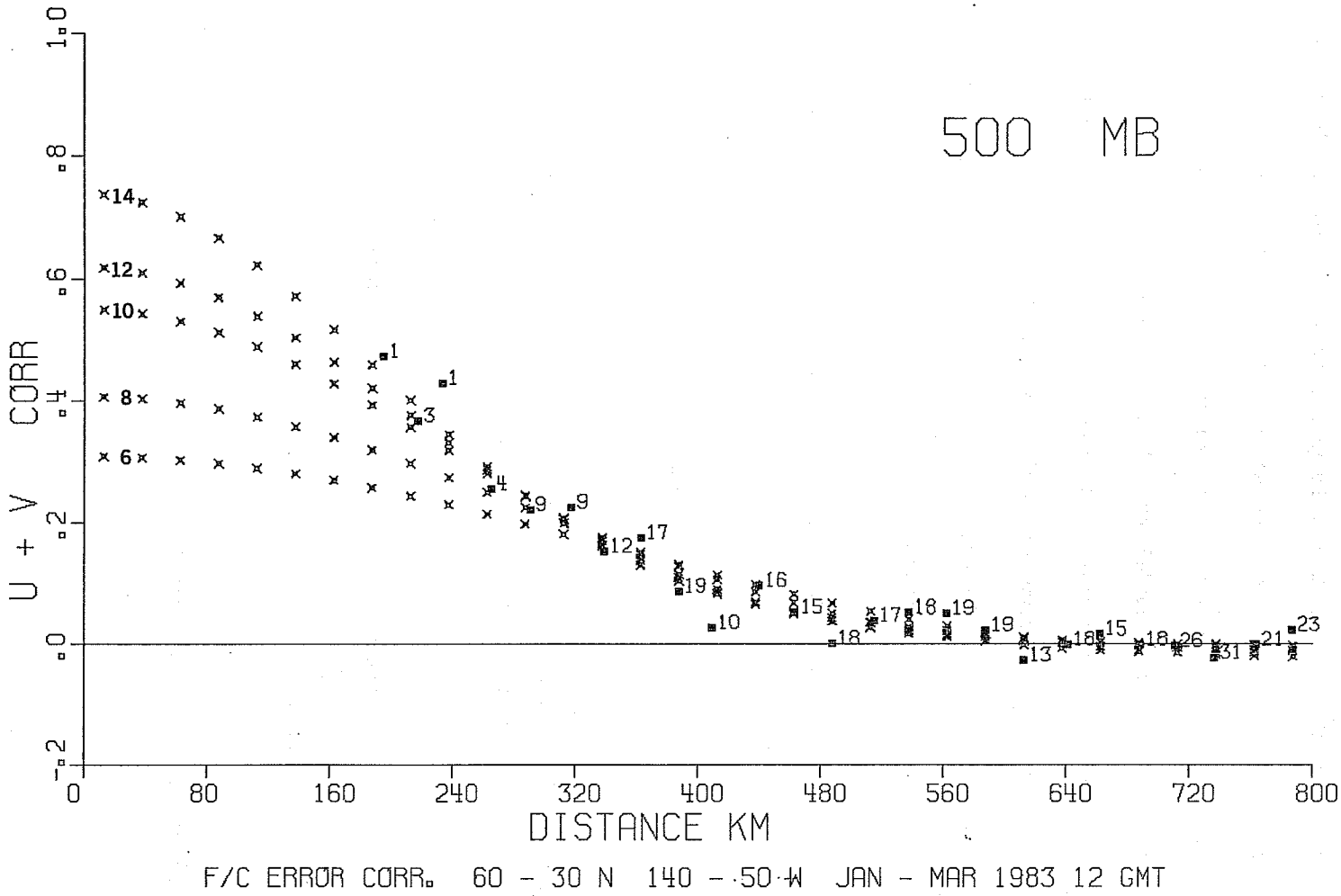

Fig. 1 The variation,at 500mb, of the <ℓ,ℓ>+<t,t> correlation with station separation: The squares show the empirically determined average value for each 25km 'bin', together with the number of station pairs in that bin. Only data for separations of 800km or less is shown. All the data out to 3000km was used in the least squares procedure to determine the five fitting curves (x) with truncations of 6, 8, 10, 12 and 14 synoptic scale terms as indicated.

A truncation of 14 terms in the synoptic-scale part of the expansion was the maximum truncation for which the least squares procedure produced physically reasonable results. The highest retained term then corresponded in scale to the shortest resolvable wavelength in the grid-point forecast model which was used in the assimilation from which the statistics are derived. Since late April 1983 the grid point model has been replaced by a spectral model with horizontal resolution T63. In this model the shortest resolvable scale would correspond to the retention of a maximum of 10 terms in the synoptic-scale part of the expansion. For this reason we decided to restrict all our results to a truncation of 10 terms in the synoptic scale components. This choice of truncation has other advantages:

- It was independent of the the presence or absence of the data from the two closest station pairs.
- It fell comfortably within the error bars of the data for the next twelve closest station pairs
- It appeared to mark an inflection point in the curves of increasing forecast error and decreasing observational error, as the truncation increased.
- The shortest resolved scale with a truncation of 10 terms has a wavelength of 584 km (Table 1). This is about twice the spacing of the closest station pairs.

5.2 Prediction error and observation error magnitudes

Fig. 3 shows the perceived rms forecast error for the vector wind together with the calculations of rms prediction error and observation error. In the

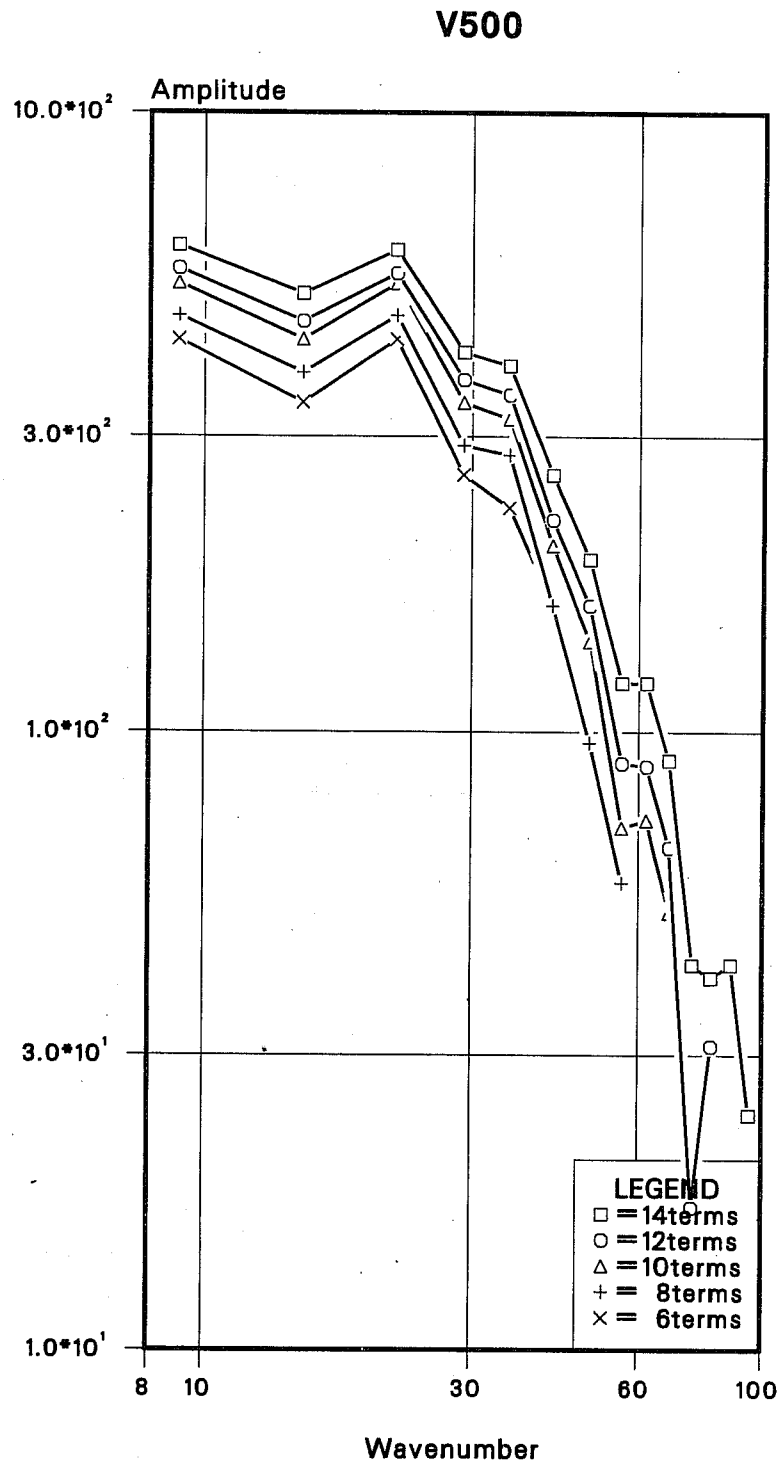

Fig. 2 The normalised spectra of the <ℓ,ℓ>+<t,t> correlation functions for truncations of 6, 8, 10, 12, and 14 terms in the least squares procedure; the truncation of each curve is indicated in the legend.

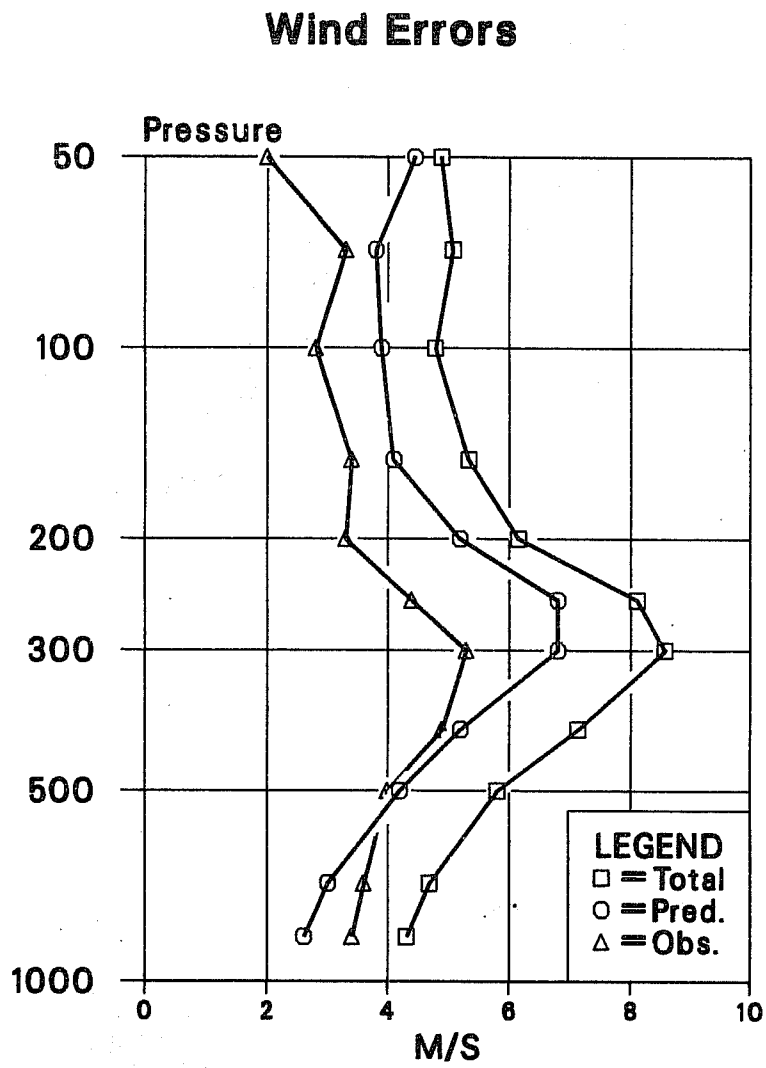

Fig. 3. The vertical variation of the perceived wind forecast errors (Total), together with the corresponding profiles of the prediction (Pred) and observation (Obs) error.

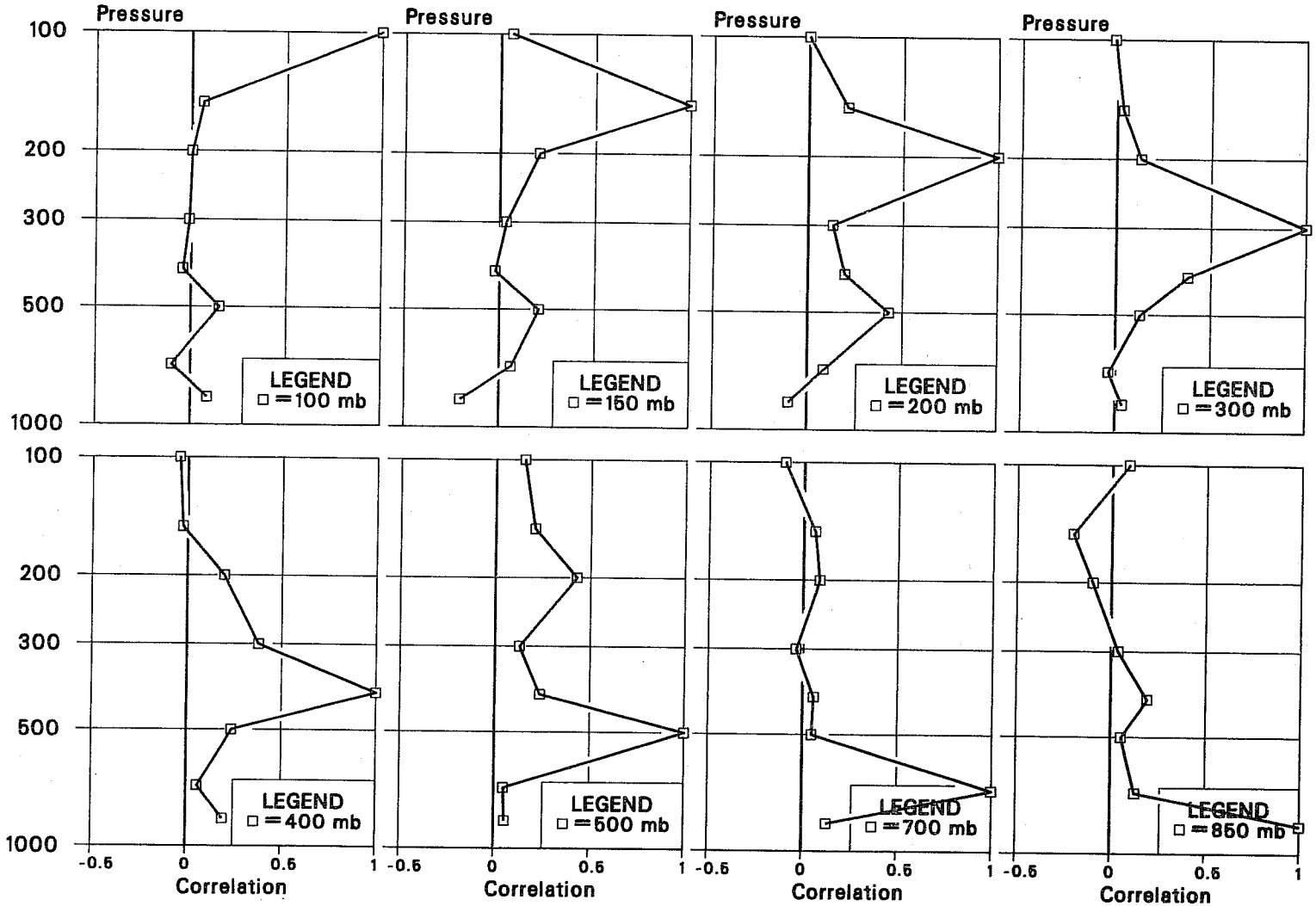

Fig. 4 Radiosonde observation error correlation for wind observations at selected standard levels, as indicated in the legend of each frame of the plot.

upper troposphere the prediction error for the vector wind is about 25% larger than the observational error; in the stratosphere the two are of the same order of magnitude; while in the lower troposphere the prediction error is some 25% smaller than the observation error. This is a result which has important implications for the ability of the assimilation system to monitor the performance of individual components of the observing system.

A useful check that the partition of perceived forecast error into prediction and observation error is reasonable is given by the estimate of the vertical correlation matrix for observational error. Fig. 4 shows plots of the columns of this matrix for a selection of levels. Since most of the North American rawinsondes use a radio-theodolite wind-finding system, there should be little vertical correlation of instrumental error between successive levels. This expectation is supported by the results of Fig. 4. Of the 55 inter-level correlations which were calculated, only one had a magnitude in excess of 0.4, two had magnitudes between 0.3 and 0.4, and nine had magnitudes between 0.2 and 0.3. These results indicate low levels of inter-level correlation of wind observational error, in accordance with expectation. Since the observational error correlation was derived as a residual from a horizontal extrapolation of horizontally correlated wind-shear errors, the good agreement with expectation gives confidence in the results.

5.3 The longitudinal and transverse wind correlations

Figs. 5 and 6 show the observational data for the longitudinal and transverse correlations, $\langle \ell,\ell \rangle$ and $\langle t,t \rangle$, at 200 mb. As discussed by Batchelor (1953)

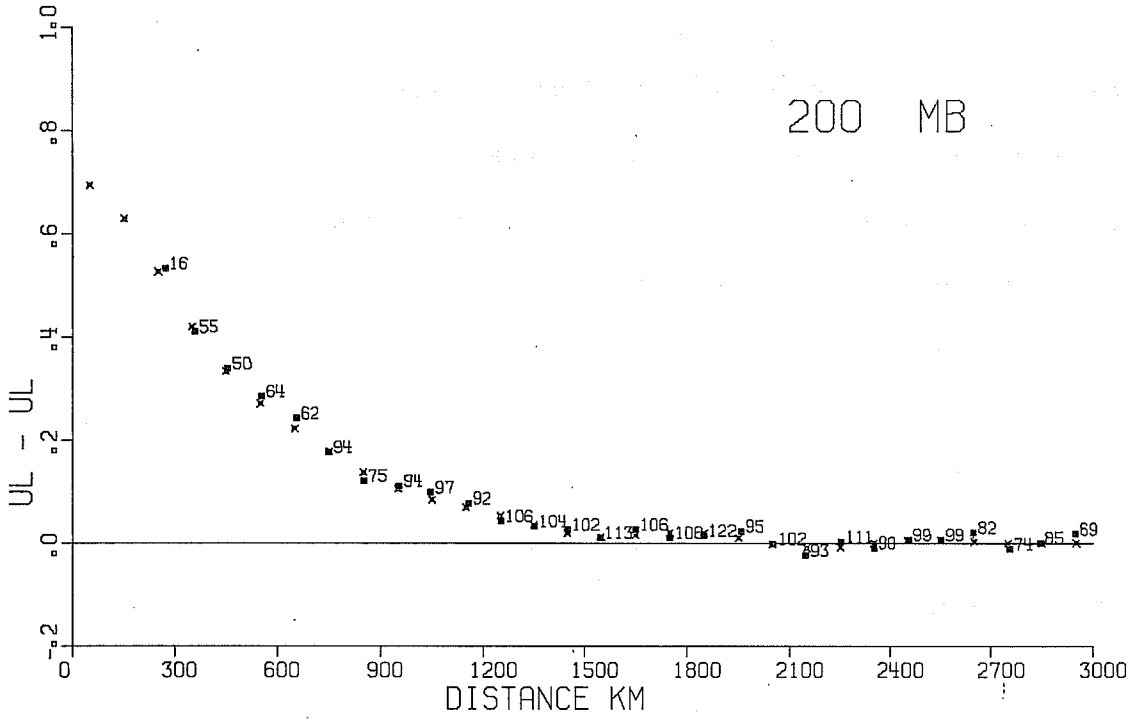

Fig. 5 The variation, at 200mb, of the $\overline{\langle \ell, \ell \rangle}$ or longitudinal correlation with station separation: The squares show the empirically determined average value for each 100km 'bin', together with the number of station pairs in that bin. All the data out to 3000km was used in the least squares procedure to determine the fitting curve (x) with a truncation of 10 synoptic scale terms.

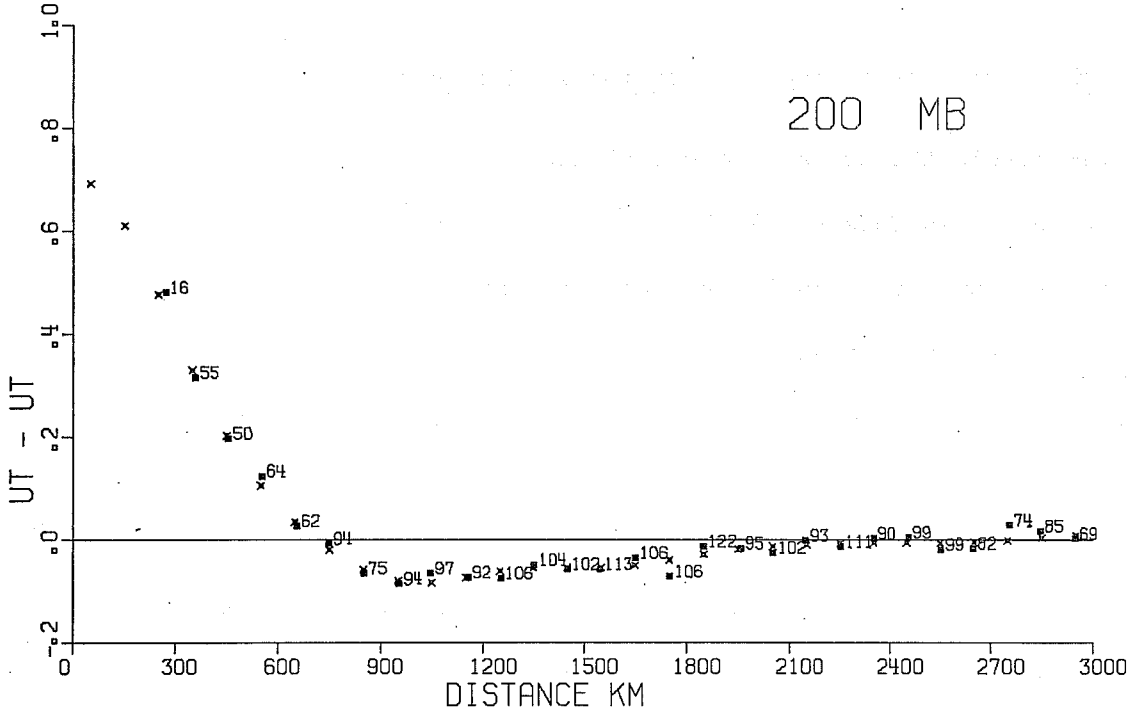

Fig. 6 The variation at 200mb of the <t,t> or transverse correlation with station separation: The squares show the empirically determined average value for each 100km 'bin', together with the number of station pairs in that bin. All the data out to 3000km was used in the least squares procedure to determine the fitting curve (x) with a truncation of 10 synoptic scale terms.

the longitudinal correlation will tend to be positive at all separations in purely non-divergent flow, while the transverse correlation is expected to change sign before approaching zero at large separations. The change of sign is due to the return flow arising from the non-divergence, as indicated in the schematic diagram in Fig. 7a.

On the other hand a purely divergent flow will tend to have a large correlation length in the transverse correlation and a short correlation length, with a change of sign, in the longitudinal direction. This is because the longitudinal flow will tend to be away from a source and towards a sink, as indicated in the schematic on Fig. 7b. The results on Figs. 5 and 6 are typical for most levels in showing a much longer correlation length for the longitudinal correlation than for the transverse correlation. This suggests, as is the case, that the forecast errors are largely non-divergent.

(a) The large scale component of the wind forecast errors

At a few levels the transverse correlation does not in fact change sign at any separation. This does not imply that the divergent and non-divergent components contribute equally to the forecast errors (Lorenc 1981, Daley 1983). In fact the constant, or large scale, component of the forecast errors is substantial, and cancels the change of sign in the transverse correlation at those levels.

Fig. 8a shows the vertical profile of the prediction error for the total wind partitioned between the synoptic-scale and large scale components, while Fig. 8b shows the vertical profile of the ratio of the large-scale component to

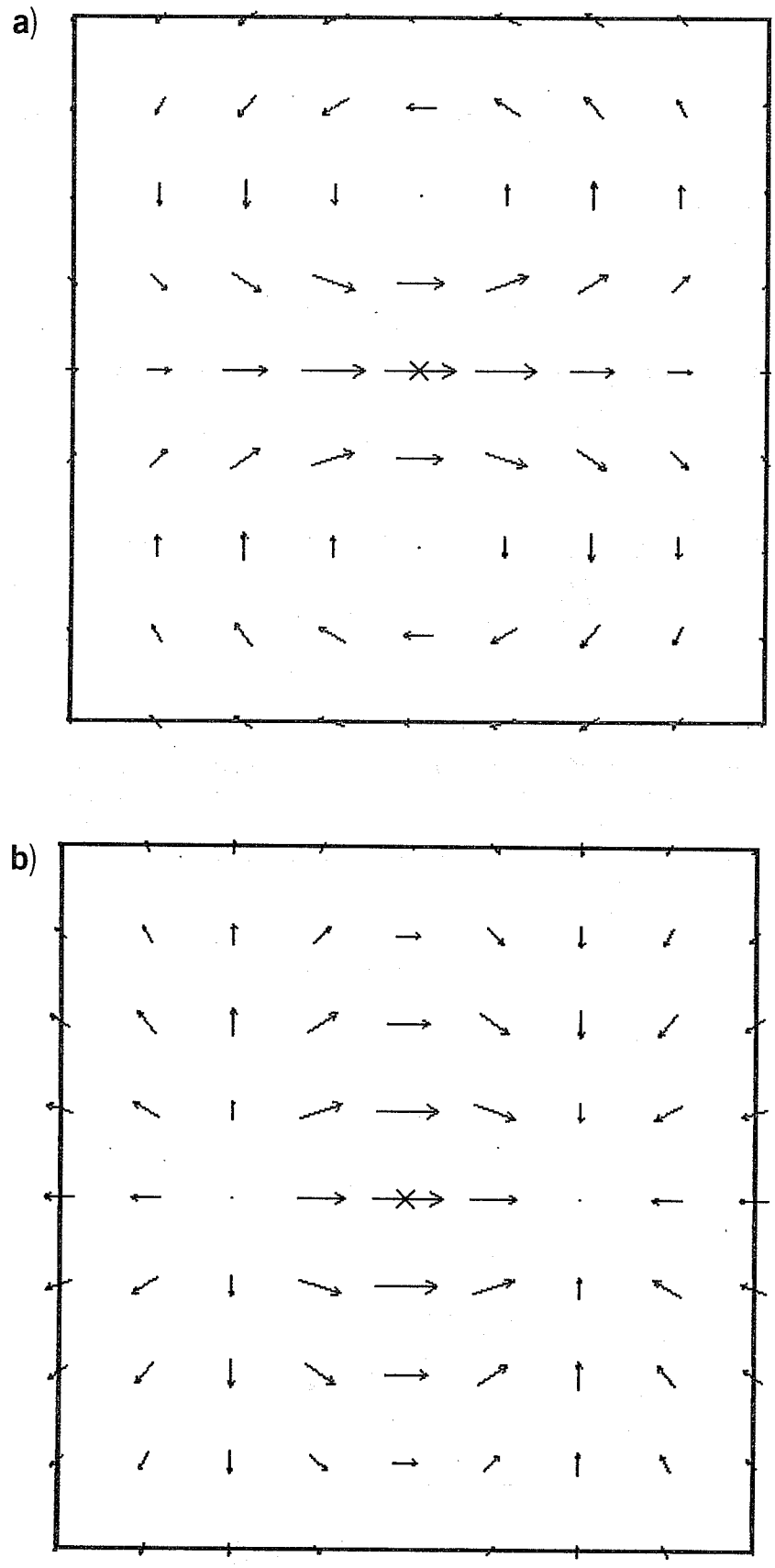

Fig. 7 Idealised schematics of the flow in the vicinity of a wind observation point X in the case where the flow is (a) purely rotational and (b) purely divergent.

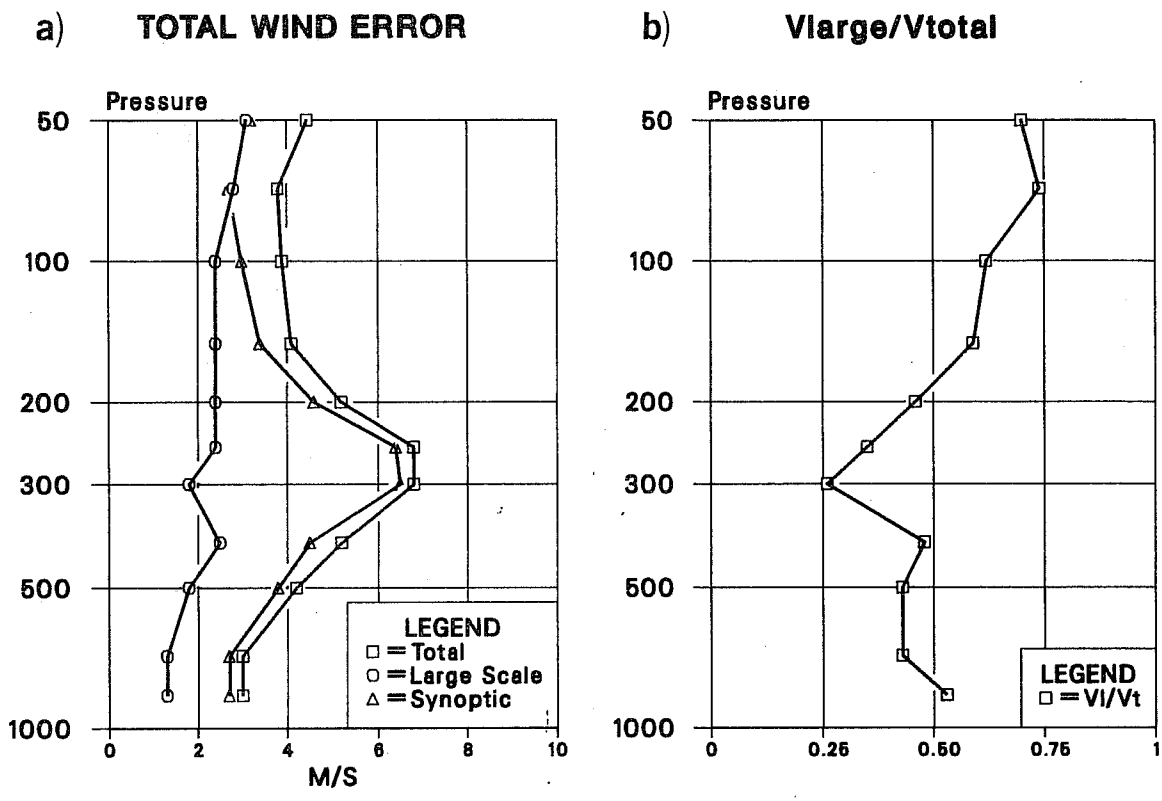

Fig. 8a: The vertical profile of the rms prediction error for vector wind (Total), together with the rms large-scale and rms synoptic-scale contributions to the total. The sum of the variances of the two contributions gives the variance of the total prediction error.
8b: the ratio of rms large-scale to rms total prediction error for vector wind.

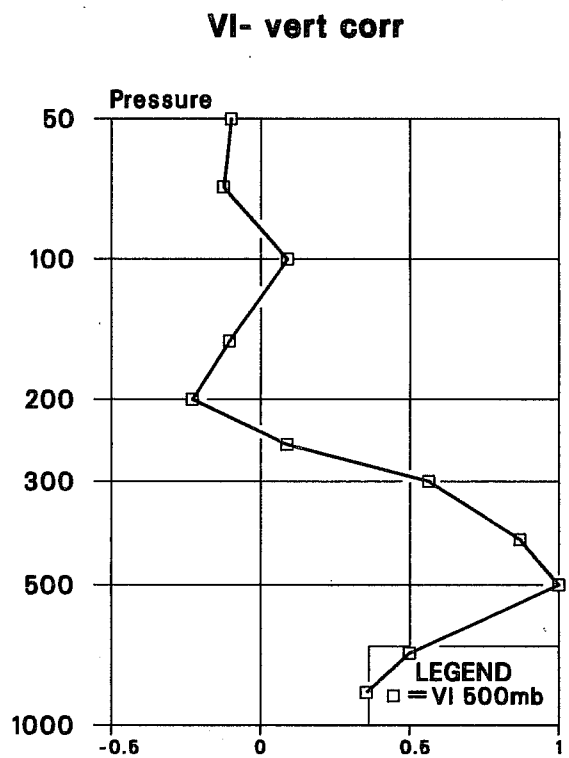

Fig. 9 The correlation with 500mb of the large scale component of the vector wind prediction error.

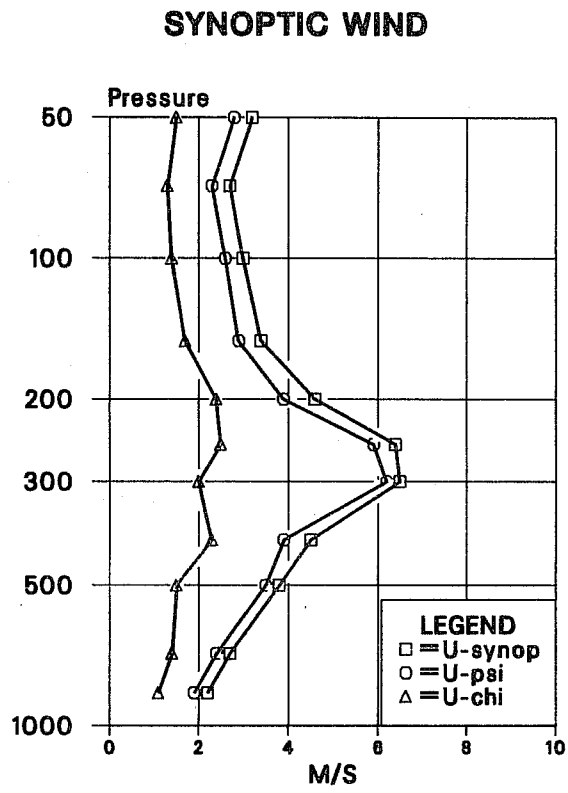

Fig. 10 The vertical profile of the rms synoptic-scale prediction error for vector wind (U-synop), together with the rms non-divergent (U-psi) and rms divergent (U-chi) contributions to the total. The sum of the variances of the two contributions gives the variance of the synoptic-scale prediction error.

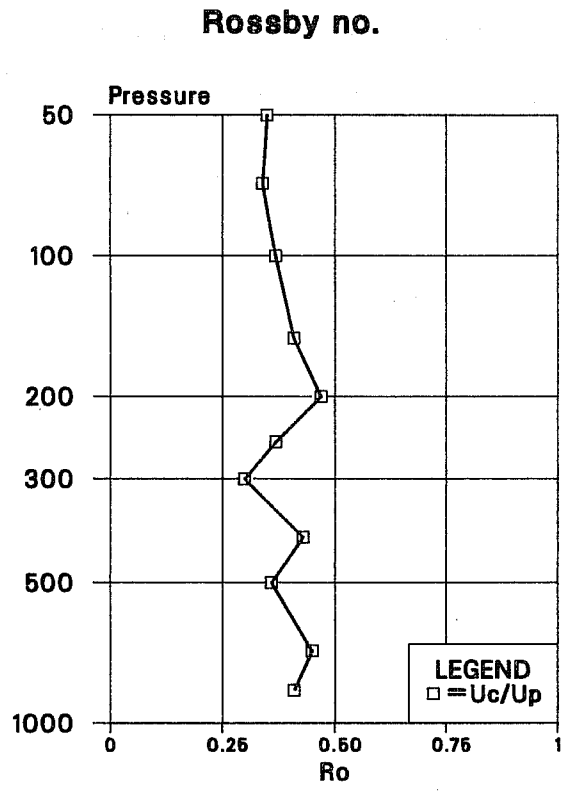

Fig. 11. The vertical profile of the Rossby number of the wind forecast errors, defined as the ratio of the rms divergent wind error to the rms prediction error, which includes both large-scale and synoptic-scale terms.

the total. At all levels except 300 and 250 mb this ratio is close to or exceeds 0.4, which is a surprisingly large figure. The large scale component at 400 mb is positively correlated with the corresponding components at all other levels, while the large-scale component at and below 500 mb tends to be negatively correlated with the same component above 250 mb. For example Fig. 9 shows the vertical correlation of the large-scale component with the 500 mb level, where the change of sign between the lower and upper troposphere is clearly apparent. These results suggest that the large-scale component of the wind forecast errors has a vertical structure corresponding to an internal mode.

(b) Synoptic scale prediction errors in the wind

Fig. 10 shows the vertical profile of the prediction error for the synoptic scale vector wind, together with the corresponding profiles for the non-divergent and divergent winds. The total prediction error is dominated by the errors in the non-divergent component. The amplitude of the forecast error in the divergent wind shows some plausible features, such as the relative maximum in the upper troposphere. The fact that it is nearly constant in the stratosphere is also interesting, and might suggest a tidal origin for the stratospheric part, since the forecast model does not have a diurnal cycle.

Fig. 11 shows the Rossby number for the forecast errors defined as $\frac{u_\chi}{u_p}$ where u_p is the rms vector wind prediction error. The Rossby number is fairly constant with height with values varying between 0.3 and 0.45. These relatively large values suggest that the forecast for the non-divergent

component of the wind is relatively more accurate than the forecast for the divergent component, leading to a larger Rossby number for the forecast errors than for the total field. The implications of the large Rossby number will be discussed in Part II when we discuss the mass-wind correlations.

5.4 Prediction and observation errors of the wind shear

Data on the thermal wind, or the vertical wind shear, has always been of great importance in manual synoptic analysis. In a multivariate objective analysis system, the weight assigned to wind shear data is determined implicitly by the vertical covariance matrices of the prediction and observation errors. The implications of the present calculations for the analysis of the wind shear are presented in Fig. 12 which shows the calculations of the prediction error and observation error for the rms vector wind shear between adjacent standard levels. According to these calculations the prediction error is lower than the observation error in the lower troposphere, 1.5 m/s/km compared with 2.5 m/s/km, while the two are of comparable magnitude in the upper troposphere and stratosphere, with peak values of order 3.5 m/s/km for both.

These results give quite an optimistic view of the accuracy of the forecasts. One would have expected the wind shear measurements to be more accurate in the troposphere than in the stratosphere. Two possible reasons may contribute to the large estimates of the observational error of the wind shear between adjacent levels in the troposphere. The variability of the shear is much greater in the troposphere than in the stratosphere. The WMO coding practice over North America is to round the wind direction to 5 degrees. With 50 m/s winds this leads to an rms rounding error of 2.2 m/s in the reported wind, and so a rounding error of 3.1 m/s in the wind difference between levels. Since

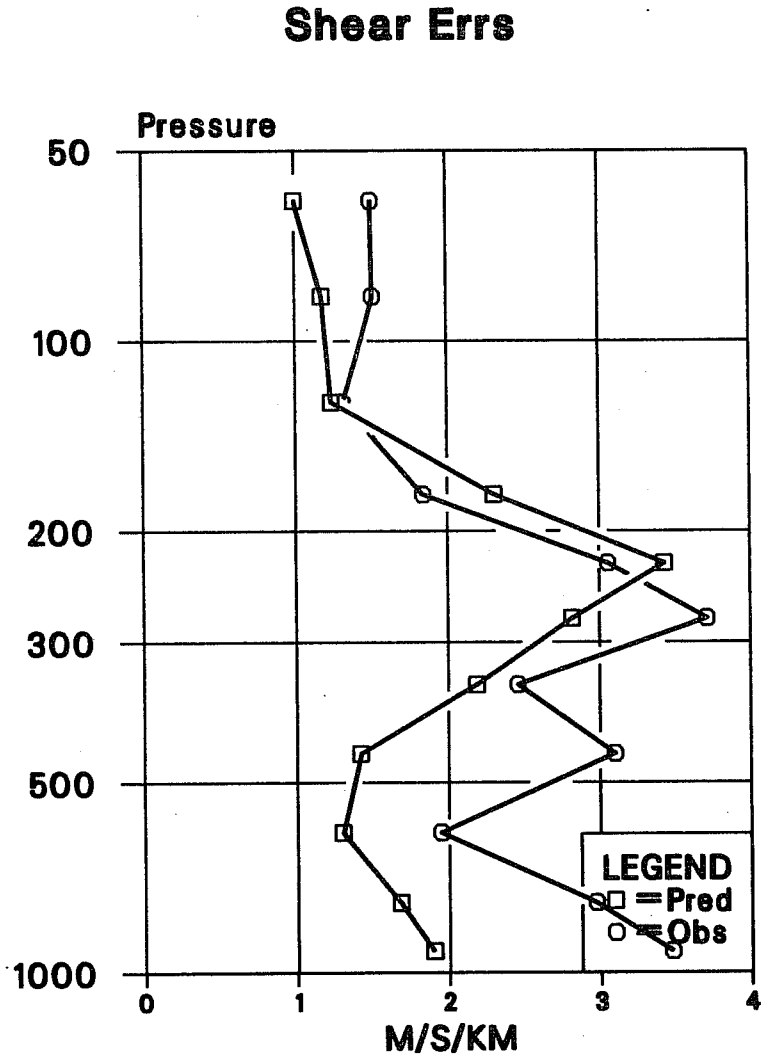

Fig. 12. Vertical profiles of the rms prediction error (Pred) and observation error (Obs) for the vertical wind shear between adjacent standard levels, in units of m/s/km.

most of the standard levels in the troposphere are separated by a vertical distance of 1 to 2 km, the estimated observational error of about 3 m/s/km is not too unreasonable in the upper troposphere.

The second possible explanation for the relatively large estimates of the observational error for the wind shear arises from the possibility of an alias of anisotropic prediction error onto the observational error. At any given analysis time it is likely that a large prediction error in the wind shear at a given point will be associated with similar errors along a particular (frontal) direction. In the isotropic calculations reported here such a configuration of prediction error could contribute to an overestimate of the horizontally uncorrelated part of the perceived forecast error, which is defined here to be the observational error.

5.5 Discussion

The partition of the perceived forecast errors into horizontally correlated prediction errors and horizontally uncorrelated observation errors results in estimates of the magnitude and vertical correlation of the observational errors which agree with expectations. Consequently the estimates of the magnitudes and vertical correlation structure of the prediction errors are probably reasonable.

Several features of the prediction errors are noteworthy. The prediction error for the wind is comparable with the observational error. The prediction error for the wind shear between adjacent standard levels is comparable with or lower than the corresponding observational error. Part of this result may

be attributable to reporting practice and perhaps also to the aliasing of anisotropic prediction error onto the observation error.

There is a substantial large-scale component in the wind prediction error, which is not represented well by a Gaussian correlation model. This component may be of even more importance in the tropics than in mid-latitudes. Over the area of study the large scale component shows an out of phase relation between the layers below 400 mb and the layers above.

6. THE ROTATIONAL WIND COMPONENT OF PREDICTION ERROR

6.1 The length scale and horizontal spectrum

Fig. 13 shows the vertical variation of the length scale of the $\langle\psi,\psi\rangle$ correlation for truncations of 6, 8 and 10 terms in the synoptic-scale components. Each truncation shows a roughly constant value for the length scale at and below 400 mb, with a marked increase with height between 400 and 150 mb. The length scale of the correlation is sensitive to the truncation in the troposphere below 300 mb, with length scales varying by 30 to 50 km as the truncation is varied. In terms of the component length scale L_c the scale varies between 400 km and about 500 km; the assimilation system which produced the statistics used a component length scale of 600 km. The length scale is rather insensitive to increases in the truncation above 6 terms for the levels above 200 mb. These results would justify a substantial increase in the horizontal resolution of the analysis system in the troposphere.

Fig. 14 shows the normalised energy spectrum of the synoptic-scale non-divergent wind errors as a function of height. At and above 200 mb the high wavenumber ends of the spectra in Fig. 14 are very steep, indicating that the largest scales (modes 1 and 2) are dominant in the stratosphere. At most levels below 250 mb the spectrum peaks at total wavenumber 15 (mode 2). The only exception is 500 mb where the spectrum peaks at total wavenumber 22 (mode 3). These results suggest that the tropospheric forecast errors in the wind field over North America are dominated by errors in the forecasts of the baroclinic waves, as might have been expected.

Balgovind et al. (1983) have investigated idealised spectra for height field forecast errors. As recognised by these authors, their proposed form for the

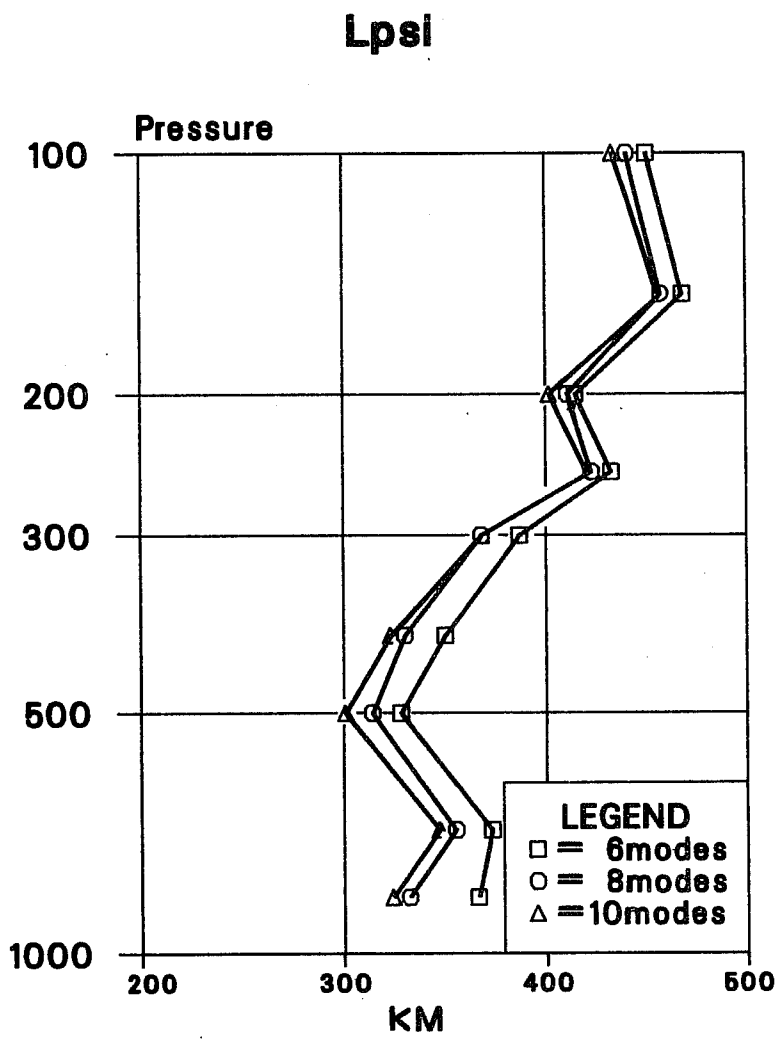

Fig. 13 Vertical profile of the horizontal length scale of the stream-function auto-correlation for three truncations in the least squares procedure, namely 6, 8, and 10 terms in the synoptic-scale components.

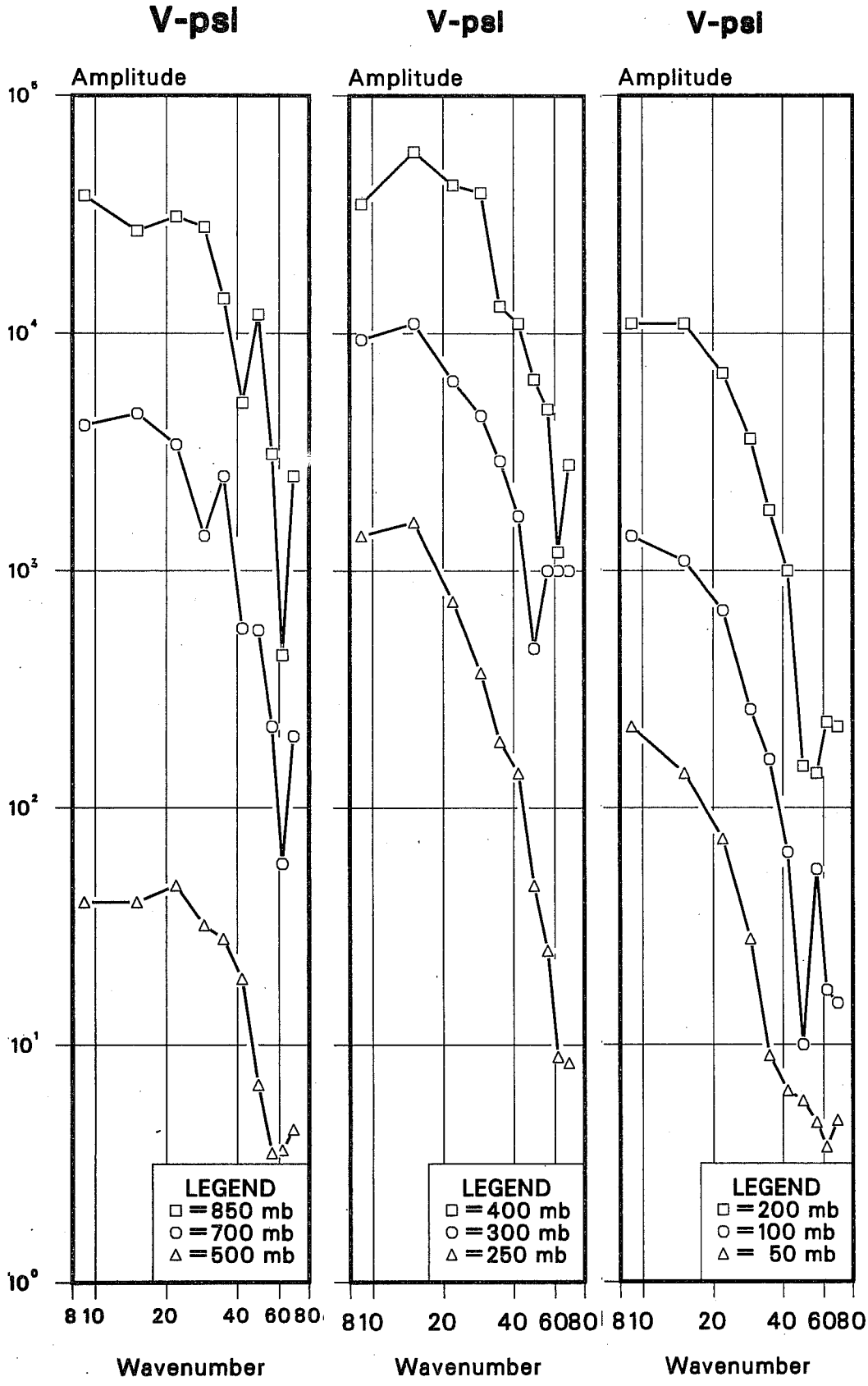

Fig. 14. Normalised energy spectra of the synoptic scale non-divergent wind forecast errors at selected levels. The unit on the ordinate is arbitrary, with horizontal lines marking the decades; the plots are separated for clarity. The unit on the abscissa is equivalent planetary wave-number. The expansions were truncated at ten terms.

stream function auto-correlation leads to a non-removable singularity at the origin in the wind-wind correlations. Their assumption about the spectrum of the non-divergent winds is not supported by the present results.

The change in the character of the spectra between the stratosphere and the troposphere is much more marked for the rotational wind field than it is for the height field. However within each region the wind spectra are fairly consistent from level to level, suggesting that separability may be a reasonably good approximation for the synoptic-scale non-divergent components of the forecast errors within each region.

The variations in the slopes of the spectra within the troposphere are of considerable interest. In the upper troposphere they seem to follow a power law that could be k^{-3} or k^{-4}, while in the lower troposphere they are much flatter. A k^{-2} spectrum is a discontinuity spectrum and there may therefore be a suggestion that the wind forecast errors are mainly associated with frontal structures in the lower troposphere, although Andrews and Hoskins (1978) suggest that frontal structures may have a $k^{-8/3}$ spectrum. We hope to pursue this question more thoroughly in later studies.

6.2 Vertical correlations

In discussing the question of separability of the rotational wind errors it is useful to consider the vertical correlations of the forecast errors. We examine the variation of the vertical correlations with horizontal mode, and compare the single mode correlations with the average correlations for the rotational wind field, and for the total wind field.

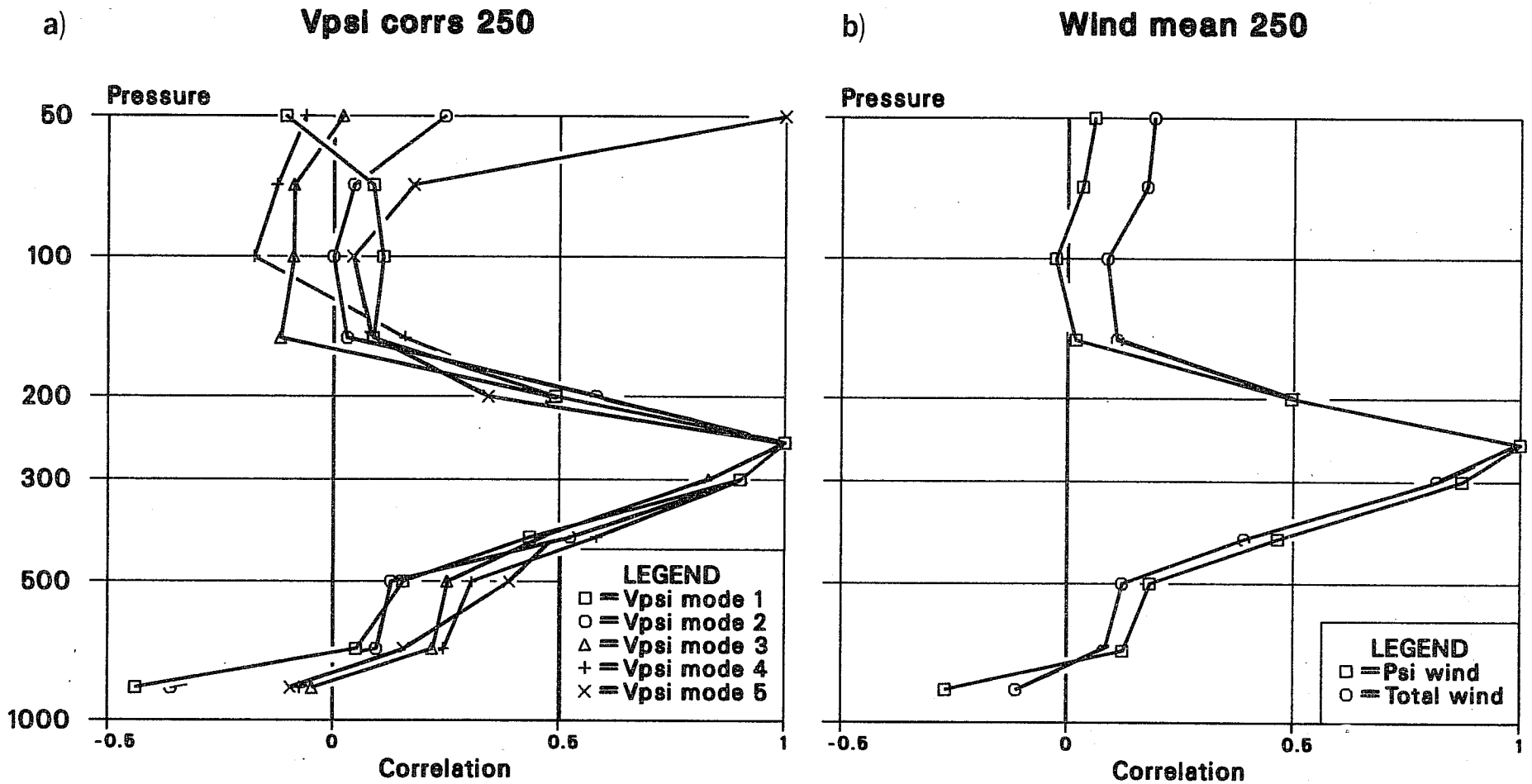

Fig. 15 a: Vertical correlations with 250mb of the first five terms in the expansion of the non-divergent wind forecast errors.

15b: Overall vertical correlations with 250mb of the non-divergent wind (Psi) and the total wind (Total).

Fig. 15a shows the vertical correlations of the first five terms of the non-divergent wind correlation with the 250 mb level. With the single exception of the correlation of mode 5 with the 50 mb level there is excellent qualitative agreement among the results, showing a short correlation length with the stratospheric layers, and a much broader correlation length in the troposphere. There is even good qualitative agreeement on the negative correlation with 850 mb. The results from other levels together with those shown in Fig. 15 suggest that separability of the non-divergent wind correlation is a good working assumption.

Fig. 15b shows the coresponding average correlations for the non-divergent wind and the total wind. The correlation length for the total wind is slightly shorter than for the non-divergent wind in the troposphere because of the form of the vertical correlation for the divergent wind, to be discussed shortly.

6.3 Parameterised vertical correlation

Fig. 16 shows the average vertical correlation of the non-divergent wind for a selected set of levels. There is a broad similarity in the shape of the curves, with a clear pattern of negative correlation between the upper and lower troposphere. The correlation between adjacent levels is of great interest for the very practical purpose of analysing strong baroclinic zones.

In order to summarise and simplify the discussion of the vertical correlation results, Fig. 17 shows a plot of the logarithm of the average vertical correlation against the difference of the logarithms of the pressure;

in effect this makes the abscissa approximately equivalent to geometric distance. The plot is made for all tropospheric levels (850 to 250 mb), and excludes negative values and all data where there is a marked increase after a steady decrease. This only happened for large vertical separations. Since practical algorithms usually try to avoid selecting data separated by more than a scale-height, these are not serious restrictions. A comparison of this plot with the equivalent result for the height field (Part II) shows that there is a very distinct difference in behaviour between the height correlations and the rotational wind correlations, with the latter being significantly sharper. This difference in vertical correlation is enhanced if the effect of the large-scale height forecast error is included. An important implication of this result is that one cannot expect the average height-stream function correlation to be extremely close to 1, since such a result would require close similarity between the vertical correlations.

For the purposes of practical analysis it is convenient to represent the correlations with a (pressure) homogeneous representation of the form

$$C = \exp\left[-\left(\frac{|\Delta \ell np|}{a_\psi}\right)^{b_\psi}\right]$$

For theoretical reasons it would be desirable to fit the data with a value of $b_\psi > 2$. This we found impossible without overestimating the correlations at short range, which would seriously underestimate the (reliably determined) thermal wind forecast errors over thin layers. For this reason a weighting

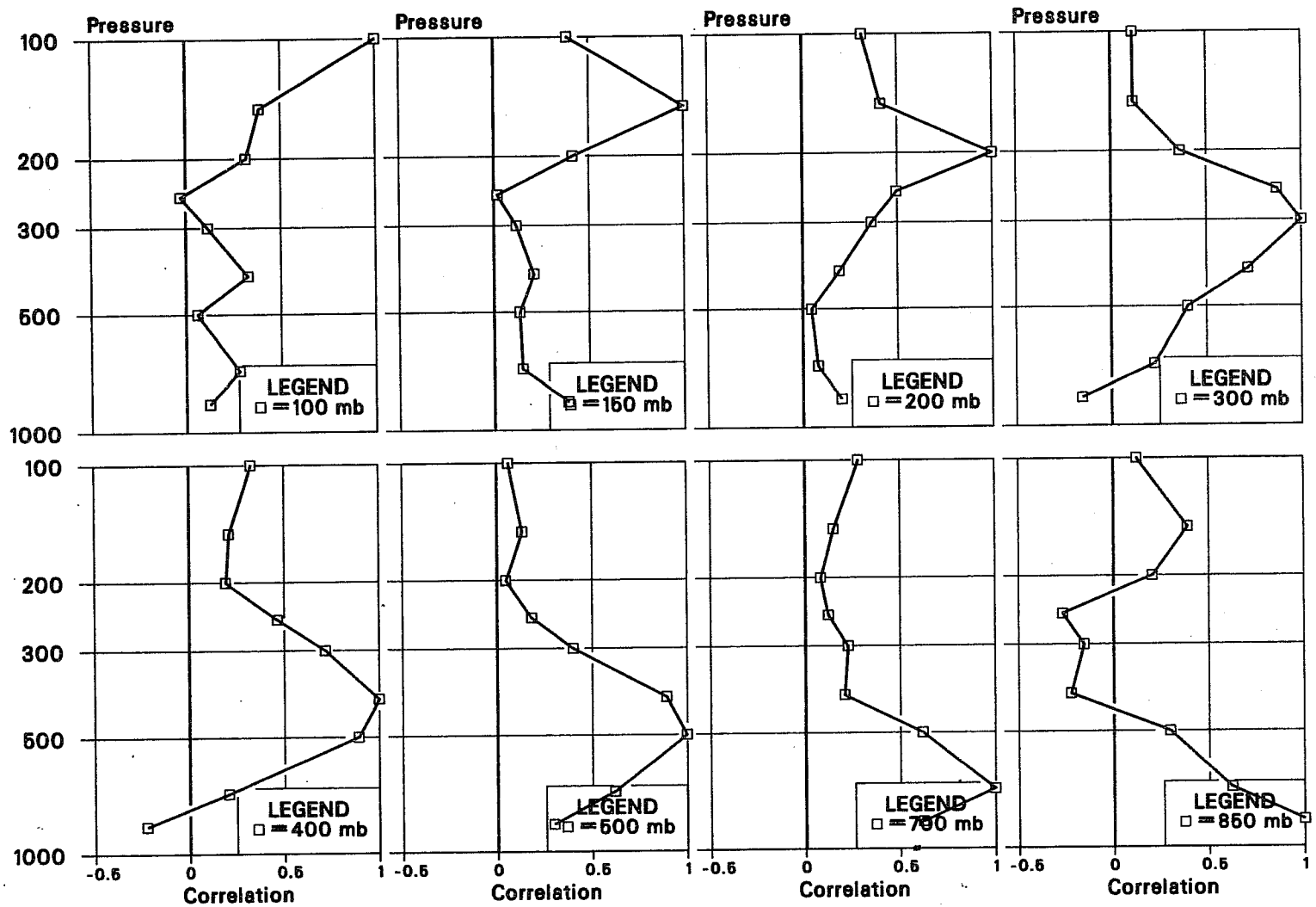

Fig. 16 Non-divergent wind prediction error vertical correlations for a selected set of standard levels, indicated in the legend of each frame of the plot. The plots corresponds to particular columns of the vertical correlation matrix for non-divergent wind.

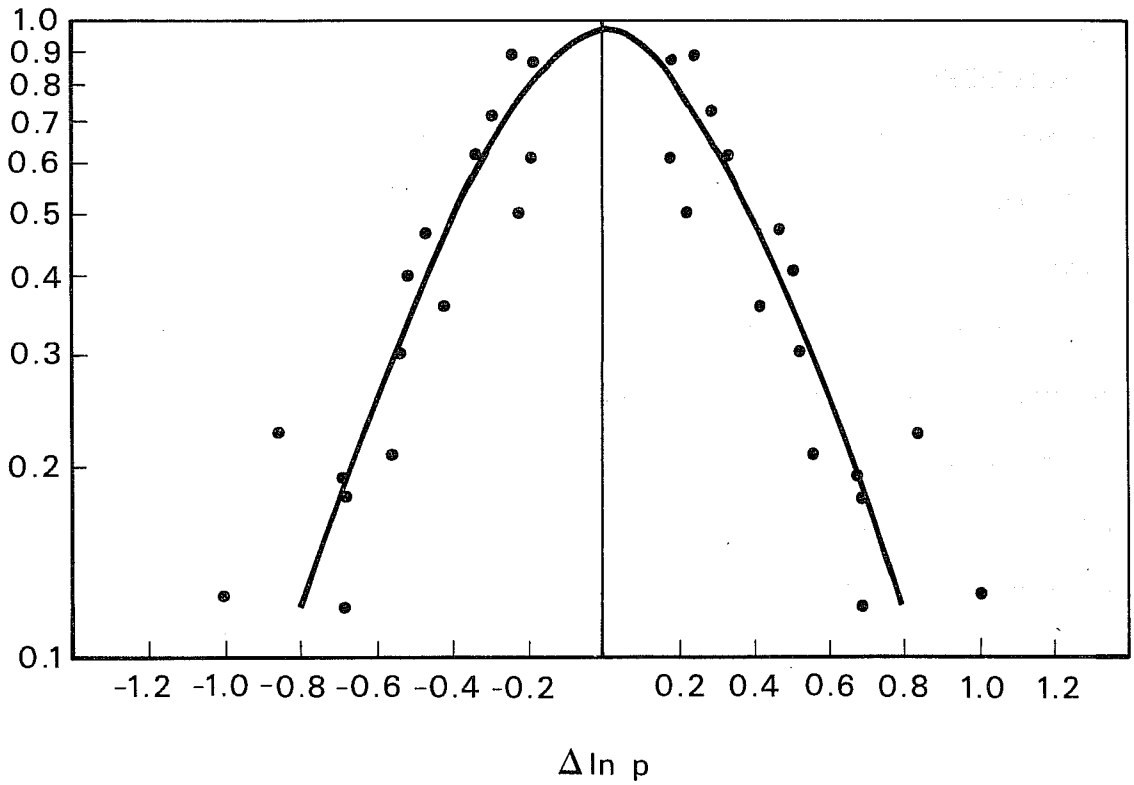

Fig. 17. Plot of the logarithm of the vertical correlation of the non-divergent wind against the difference in the logarithms of the pressures of the levels involved in the correlation. The selection of the pairs of levels is described in the text. The curve representing the simplified parameterisation of the correlation data is also described in the text.

which respected the data for short separations was used. It was found that $b_\psi = 1.6$ gave the best fit. A similar result was found for the height field. The value of a_ψ was found to be 0.5; the correlation therefore decreases to e^{-1} for a separation of half a scale height. This curve is shown in Fig.17 and it gives a reasonable representation of the data.

6.4 Discussion

The horizontal length scale of the streamfunction correlation is markedly larger in the stratosphere than in the troposphere. The length scales are sensitive to resolution, and the results would justify an increase in the horizontal resolution of the analysis. The vertical correlation structure is nearly independent of horizontal mode for the (dominant) first five modes. This suggests that separability is a good working assumption for the streamfunction errors. Although the vertical correlations are not homogeneous in the troposphere, they can be represented reasonably well by a homogeneous function provided the vertical separation is not too large.

7. THE DIVERGENT WIND COMPONENT OF PREDICTION ERROR

7.1 Horizontal spectrum

Fig. 18 shows the normalised spectrum of the divergent wind forecast error as a function of height. At all levels except 300 mb the spectrum is dominated by the gravest horizontal mode. The fact that the tails of the spectra are noisy in the troposphere does not mask the dominance of the large scale modes.

7.2 Vertical correlation of divergent wind errors

The forecast errors in the divergent wind seem to occur for different reasons in the stratosphere and the troposphere. Fig. 19 shows the vertical correlation for the gravest horizontal mode for a selection of levels. This mode dominates the kinetic energy of the divergent wind. Fig. 19 shows that there are strong negative correlations of the wind errors within the troposphere, which would be consistent with the view that this component of the error is associated with baroclinic processes in the troposphere. Similar structures are found in the vertical correlations of mode 2. The correlations between the stratospheric and tropospheric levels are low and apparently noisy, while correlations within the stratosphere are always positive. We interpret these results as suggesting that the stratospheric component of the divergent wind error is of different, and possibly tidal, origin. This interpretation will be discussed when considering the height-wind correlations in Part II.

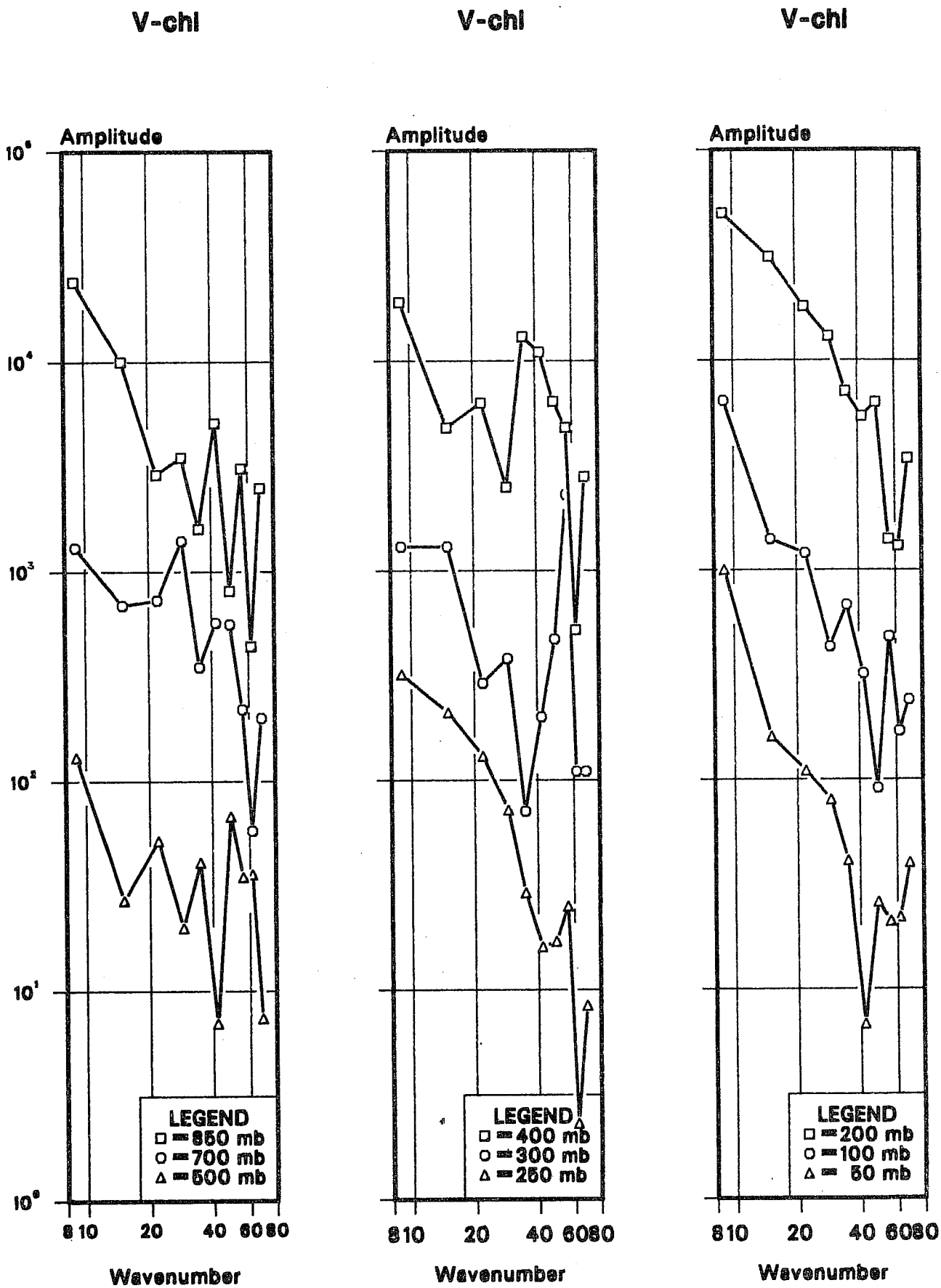

Fig. 18. Spectra, as Figure 14, of the divergent component of the wind forecast errors.

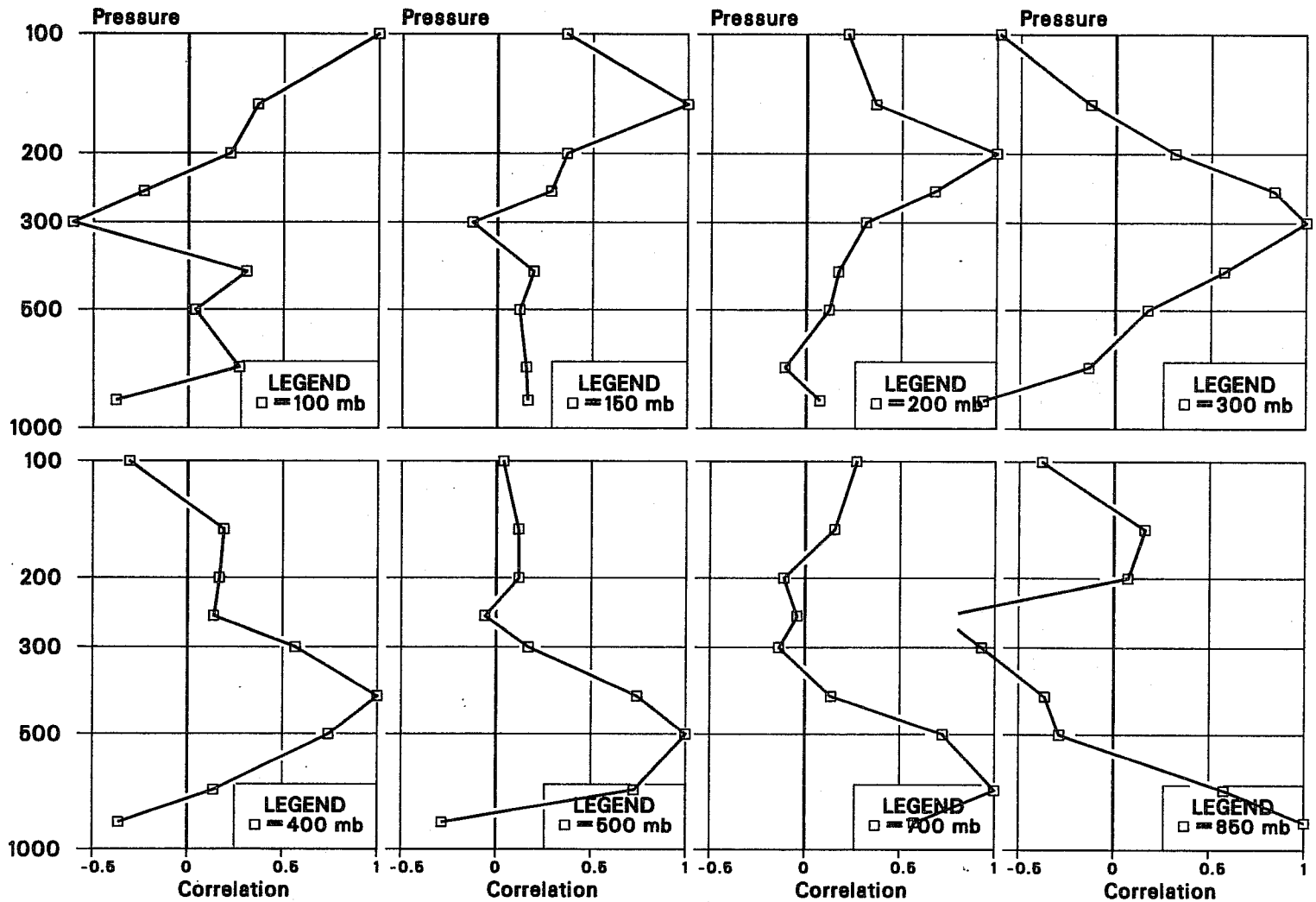

Fig. 19 As figure 16 for the first term in the expansion of the divergent wind forecast errors.

7.3 The stream function-velocity potential correlation

Fig. 20 shows a plot of the $\langle\psi,\chi\rangle$ correlation for the first mode, as a function of height. The magnitude of the correlation is less than 0.097 at all levels except 700 and 70 mb, where it has values of -.219 and .109 respectively.

At almost all levels the spectrum of H is dominated by the first mode. The only exceptions of any significance are the 300 and 250 mb levels where modes 1 and 2 are comparable. A similar feature was noted already in the spectrum of the $\langle\chi,\chi\rangle$ correlation.

Given such very low correlations it would probably be sensible to suppose that the figure merely shows noise in the calculation of a quantity whose true value is zero. If this were indeed the case then one might conclude that the conditions for Obukhov's theorem, on the independence of rotational and irrotational flow velocities in isotropic flow, were indeed satisfied by the forecast errors. On the other hand one could argue that the structure shown in the figure is too smooth to be merely noise, particularly below 200 mb. We see a clear distinction between the upper and lower troposphere in the sign of the correlation. Whichever viewpoint is true, the matter is only of academic interest. As pointed out by Daley (1983), the correlation is of little consequence for practical analysis unless it is reasonably close to 1.

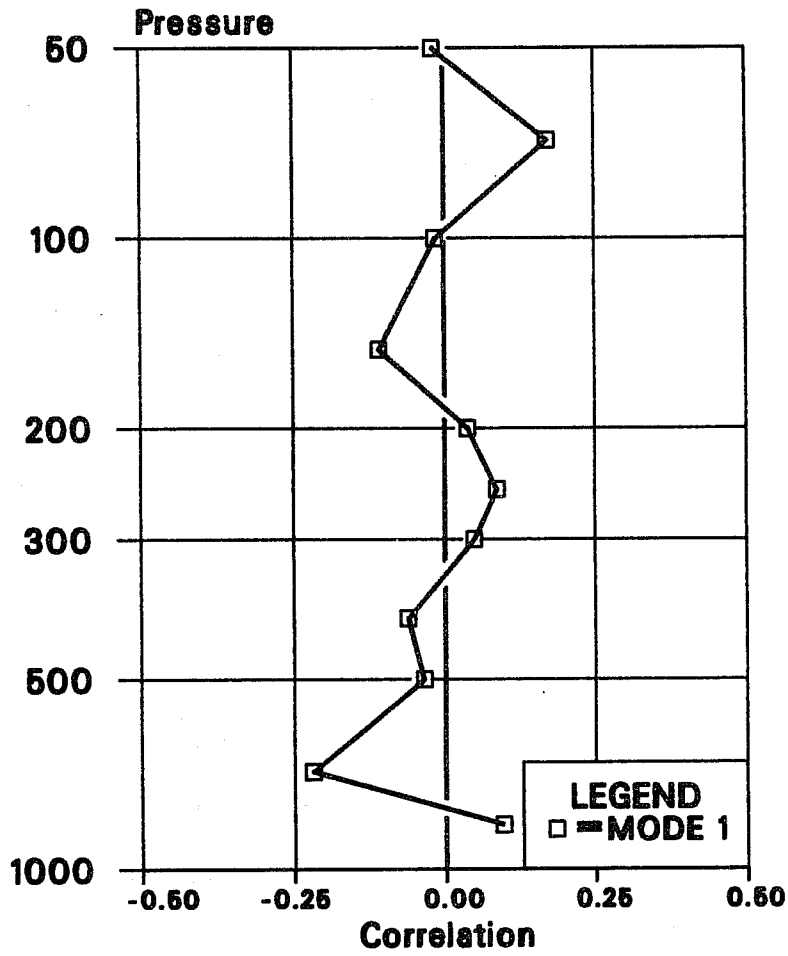

Fig. 20 Vertical profile of the streamfunction velocity potential correlation for the gravest synoptic scale term in the expansion of the correlation.

8. SUMMARY AND CONCLUSIONS

The methods developed in this paper provide a comprehensive three-dimensional and spectral description of the covariance structure of the wind forecast and wind observation errors, subject only to the assumption of local homogeneity of the errors. The requirements of positive-definiteness on the spectra of the correlation functions guarantees the positive-definiteness of any Optimum Interpolation analysis matrix generated from the functional representations. This is essential in both theoretical and practical work.

The mathematical formulation which is used to estimate the $\langle\psi,\psi\rangle$, $\langle\chi,\chi\rangle$ and $\langle\psi,\chi\rangle$ covariances from the empirically determined $\langle u,u\rangle$, $\langle v,v\rangle$, and $\langle u,v\rangle$ covariances is sufficiently general to determine both the isotropic and anisotropic components of the prediction error. The present study deals only with the isotropic components.

The wind forecast errors are dominated by the synoptic scale stream function component, although there is also a large-scale component whose vertical structure appears to be internal; the divergent component of the wind errors is about the same magnitude as the large-scale component in the troposphere and rather smaller in the stratosphere.

The forecast errors in the wind field are comparable in magnitude with the observation errors. The errors in the forecasts of the vertical wind shear also appear to be comparable with the observational errors. The term observational error in our discussion includes sampling errors as well as instrumental error.

There are good grounds for increasing the resolution of our analysis system, both in the horizontal and vertical.

The synoptic scale wind field forecast errors have been resolved into rotational and divergent components. The Rossby number of the wind forecast errors (defined as the ratio of the divergent to the total wind amplitude) is between 0.3 and 0.45 at all levels. The errors in the divergent wind field are of large horizontal scale. The stratospheric component of these errors possibly arises from the absence of a diurnal tide in the forecast model. The tropospheric divergent wind errors have a vertical correlation structure which is consistent with a purely tropospheric origin for the errors.

The largest wind forecast errors occur in the rotational component of the flow. The horizontal and vertical scales of the $\langle\psi,\psi\rangle$ correlation would justify a marked increase in the resolution of the analysis system. This would probably have a significant impact on the thermal wind analysis. The $\langle\chi,\psi\rangle$ correlation is quite weak.

The methods and results presented above can be extended in a variety of directions. Current studies are concerned with the forecast errors in the tropics, and anisotropic aspects of the forecast errors. The indications that the accuracy of the forecast is frequently comparable with that of the observations offers considerable potential for monitoring the performance of both the observational system and the analysis system (Hollingsworth et al. 1985a). Finally, the methods can be adapted to provide spectral estimates of analysis accuracy.

ACKNOWLEDGEMENTS

We are grateful to our colleagues at ECMWF for many discussions and helpful comments, particularly D.B.Shaw, G.J.Cats, D.M.Burridge and A.J.Simmons. R.Daley and N.A.Phillips provided much stimulation through early access to their work. H.Tennekes and A.C.Wiin-Nielsen provided valuable guidance to the literature. We are particularly grateful to I. Rhodes for her skill and patience in taking the manuscript through many iterations.

REFERENCES

Andrews D.G. and B.J.Hoskins 1978: Energy spectra predicted by semi-geostrophic theories of fronto-genesis J.Atmos.Sci. 35, 509-512

Arpe K., A. Hollingsworth, A.C. Lorenc, M.S. Tracton, S. Uppala, P. Kallberg 1985: The response of Numerical Weather prediction Systems to FGGE II-b Data, Part II: Forecast Verifications and Implications for Predictability. Quart.J.Roy.Meteor.Soc. 111, 67-102

Balgovind, R., M. Ghil, A. Dalcher and E. Kalnay, 1983: A stochastic-dynamic model for the spatial structure of forecast error statistics. Mon.Wea.Rev., 111, 701-722.

Batchelor, G.K. 1953: The Theory of Homogeneous Turbulence. Cambridge University Press pp197

Bengtsson, L., M. Kanamitsu, P. Kallberg and S. Uppala, 1982: FGGE 4-dimensional data assimilation at ECMWF. Bull.Amer.Met.Soc., 63, 29-43.

Bergman, K.H. 1979: Multivariate analysis of temperatures and winds using optimum interpolation. Mon.Wea.Rev., 107, 1423-1444.

Bjorheim K., P. Julian, M.Kanamitsu, P.Kallberg, P.Price 1981: FGGE III-b Daily Global Analyses. Available from ECMWF

Brown P S and G.D. Robinson, 1979: The variance spectrum of tropospheric winds over Eastern Europe. J.Atmos.Sci. 36, 270-286

Buell, C.E. 1971: Two-point wind correlations on an isobaric surface in a nonhomogeneous non-isotropic atmosphere. J.Appl.Met., 10, 1266-1274.

Buell, C.E. 1972: Correlation functions for wind and geopotential on isobaric surfaces. J.Appl.Met., 11, 51-59.

Buell, C.E. and Seaman, R.S. 1983: The 'scissors' effect: anisotropic and ageostrophic influences on wind correlation coefficients. Aust.Met.Mag., 31, 77-83.

Burridge,D.M. and J. Haseler 1977: A model for medium range weather prediction ECMWF Tech.Rep. No. 4.

Cats, G.J., and W. Wergen, 1982: Analyses of large-scale normal modes by the ECMWF analysis scheme. ECMWF Workshop on Current Problems in Data Assimilation.

Daley, R. 1983: Spectral characteristics of the ECMWF objective analysis system. ECMWF Tech. Rep. No. 40, 119 pp.

Fisher, R.A., 1921: On the probable error of a correlation deduced from a small sample. Metron., 1, Part 4, 3-32.

Gandin, L.S. 1963: Objective analysis of meteorological fields. Translated from Russian by the Israeli Program for Scientific Translations (1965).

Gustavsson N. 1981: 'A review of methods for objective analysis' in Dynamic meteorology- Data assimilation methods, ed. L. Bengtsson, M. Ghil and E.Källén Pub.Springer-Verlag.

Hildebrand F.B. 1962: Advanced calculus for applications. Prentice Hall 646pp.

Hollett, S.R. 1975: 3 dimensional spatial correlations of PE forecast errors. M.Sc. thesis. Department of meteorology, McGill University, Montreal, Canada. 73 pp.

Hollingsworth A., D.B.Shaw, P.Lönnberg, L.Illari, K.Arpe, A.J.Simmons 1985a: Monitoring of Observation quality by a data assimilation system. To appear.

Hollingsworth A., A.C.Lorenc, M.S.Tracton, K.Arpe, G.Cats, S.Uppala, P.Kallberg 1985b: The response of Numerical Weather prediction Systems to FGGE II-b Data Part I : Analyses. Quart J Roy Meteor Soc 111, 1-66

Hutchings, J.W. 1955: Turbulence theory applied to large-scale atmospheric phenomena. J.Met., 12, 263-271.

Julian, P.R. and H.J. Thiebaux, 1975: On some properties of correlation functions used in optimum interpolation schemes. Mon.Wea.Rev., 103, 605-616.

von Karman T., L. Howarth, 1938: On the statistical theory of isotropic turbulence. Proc.Roy.Soc.A, 164, 192-.

Khinchin A.Y. 1934: Korrelationstheorie der stationaren stochastischen Prozesse, Math.Ann.109 No.4, 604-615.

Lönnberg P., A.Hollingsworth 1985: The statistical structure of short range forecast errors as determined from radiosonde data, Part II: Covariance of height and wind errors. To appear

Lorenc, A.C. 1981: A global three-dimensional multivariate statistical interpolation scheme. Mon.Wea.Rev., 109, 701-721.

Machenhauer, B. 1977: On the dynamics of gravity oscillations in a shallow water model, with application to normal mode initialisation. Contrib.Atmos. Phys., 50, 253-271.

Obukhov A.M. 1954: Statistical description of continuous fields. Trudy Geofiz In-ta Akad Nauk SSSR No 24(151) 3-42. English translation by Liaison Office, Technical Information Centre, Wright-Patterson AFB F-TS-9295/v.

Panchev, S. 1971: Random functions and turbulence. Pergamon Press 444pp.

Phillips, N.A. 1982: On the completeness of multi-variate optimum interpolation for large-scale meteorological analysis. Mon.Wea.Rev., 110, 1329-1334.

Rutherford, I.D. 1972: Data assimilation by statistical interpolation of forecast error fields. J.Atm.Sci., 29, 809-815.

Schlatter, T.W. 1975: Some experiments with a multivariate statistical objective analysis scheme. Mon.Wea.Rev., 103, 246-257.

Seaman, R.S. 1977: Absolute and differential accuracy of analyses achievable with specified observational network characteristics. Mon.Wea.Rev., 105, 1211-1222.

Temperton C. D.L. Williamson 1981: Normal mode initialisation for a multilevel grid-point model Part I : Linear Aspects Mon.Wea.Rev., 109, 729-743.

Tiedtke M., J.F. Geleyn, A. Hollingsworth, J.F. Louis 1979: ECMWF model parameterisation of sub grid scale processes. ECMWF Tech.Rept.No.10.

Williamson D.L., C.Temperton, 1981: Normal mode initialisation for a multi-level grid-point model, Part II: Nonlinear aspects Mon.Wea.Rev., 109, 744-757.

Zlotnicki, V., B. Parsons, C. Wunsch, 1982: The inverse problem of constructing a gravimetric geoid. J.Geophy.Res., 87, 1835-1848.